CONFIDENTIAL

RESEARCH MEMORANDUM

A FLIGHT AND ANALYTICAL STUDY OF METHODS FOR REDUCING AUTOMATIC-INTERCEPTOR TRACKING ERRORS CAUSED BY TARGET MANEUVERS

By Charles W. Mathews, Donald C. Cheatham, and Howard C. Kyle

Langley Aeronautical Laboratory
Langley Field, Va.

CLASSIFIED DOCUMENT

NATIONAL ADVISORY COMMITTEE FOR AERONAUTICS

WASHINGTON

September 28, 1956

CONFIDENTIAL

NATIONAL ADVISORY COMMITTEE FOR AERONAUTICS

RESEARCH MEMORANDUM

A FLIGHT AND ANALYTICAL STUDY OF METHODS FOR REDUCING AUTOMATIC-INTERCEPTOR TRACKING ERRORS CAUSED BY TARGET MANEUVERS

By Charles W. Mathews, Donald C. Cheatham, and Howard C. Kyle

SUMMARY

The present study is concerned primarily with methods of reducing or eliminating automatic-interceptor tracking errors that are caused by target maneuvers. The flight-test phase of the study was made with an automatic interceptor system. This system utilized an error integrator in the deflection channel of the automatic system to eliminate steady-state errors caused by steady target maneuvers.

Flight tests of the original system showed that large peak errors and long transient times resulted when the system attempted to track a target entering a steady turn. Attempts to improve this tracking performance by gain adjustments were unsuccessful because of adverse effects on system stability.

Comparisons by means of a simplified analytical study of the original system with two systems having alternate methods of eliminating steady-state errors indicate that one of the alternate systems, referred to as the system with filtered input differentiation, was capable of improved performance. This system was mechanized in the interceptor and flight tested. The results showed considerable reduction in the duration and peak of the transient errors following a target turn entry.

INTRODUCTION

The reduction or elimination of steady-state errors is frequently an important consideration in the design of servomechanisms. The most widely used approach to the elimination of these errors is through use of integration of the error signal (or its effective equivalent; namely, cancellation of the feedback of the output). This approach detrimentally affects the stability of the system, and therefore steady-state errors

must be reduced over moderately long times compared with the natural period of the system. (See ref. 1.)

A problem of this type is frequently encountered during the attack operation of an automatic interceptor whenever the target performs steady turns or pull-ups. Under such conditions a steady-state error often results from the use of some feedback quantity in the autopilot which does not go to zero under steady maneuvering conditions. This feedback quantity may be needed for stability and therefore cannot be eliminated. For example, a bank-angle signal is a frequently used feedback in the aileron channel of autopilot systems. Since a steady bank angle other than zero exists in a turn, the bank-angle-feedback signal generated under these conditions needs to be canceled if zero aiming error is to be maintained. Although error integration often is used as a source of this canceling signal, it is not completely satisfactory because of its effect on system stability, particularly in systems having fairly long natural periods such as characterize the outermost loop of an interceptor system. Reference 2 presents an analog study of an automatic interceptor system where this problem was encountered.

This problem was also encountered in an automatic interceptor system that was assigned to the National Advisory Committee for Aeronautics for study of automatic-interceptor flight control. This system utilized error integration in the deflection channel to eliminate steady-state errors in turns. Results of initial flights indicated that the peak magnitudes and the transition times of the deflection error following a target turn were excessive. Alleviation of this condition by increases in the gains of the error or error integral signal was precluded by detrimental effects on system stability, and it appeared worthwhile to consider alternate means for elimination of steady-state errors.

Two other systems designed to eliminate steady-state errors were analyzed as to their usefulness and limitations, and one of these systems was mechanized into the automatic interceptor system for purposes of flight check. This paper presents results of the analysis and of the flight tests.

SYMBOLS

A	constant
a_B	acceleration of target in plane of wings of interceptor, ft/sec^2
a_F	acceleration of interceptor, ft/sec^2

G	constant for linear approximation of sine function, 0.86/radian
g	acceleration of gravity, 32.2 ft/sec^2
K	loop gain
p	Laplace operator, per sec
R	range, ft
t	time, sec
V	velocity, ft/sec
β	coefficient of frequency-variant term of approximation of power spectral density of radar noise
δ	control-surface deflection, radians
ϵ	error voltage
θ	pitch angle, radians
σ	tracking error, angle between gun line and line of sight, radians except where specified in mils
τ	time constant, sec
ϕ	roll (or bank) angle, radians
ψ	yaw angle, radians
ω	rate of angular rotation, radians/sec

Subscripts:

a	airplane or aileron
D	differentiator
e	elevator
f	filter
I	integrator
i	input
m	maximum value

LS line of sight

n noise

o output

(o) initial condition

p Laplace operator

σ tracking error

ϕ roll angle

A bar over a quantity indicates the smoothed (filtered) value.

A dot over a quantity indicates differentiation with respect to time.

DESCRIPTION OF AUTOMATIC INTERCEPTOR SYSTEM

General

The automatic interceptor system consisted of a radar fire-control system, a tie-in, and an automatic pilot installed in a jet fighter airplane having unswept wings. A photograph of the airplane is presented in figure 1, and its dimensional and mass characteristics are presented in table I. Reference 3 is a report covering the stability characteristics of this airplane.

The automatic interceptor utilized a radar fire-control system already installed in the production version of the airplane. This fire-control system was designed for human-pilot operation using a radarscope display. A photograph of the fire-control system is presented in figure 2 and the tracking performance of the radar is discussed in reference 4. The fire-control computer provided the lead-angle information required to fly lead-pursuit trajectories.

The tie-in is essentially a computing system which ties the fire-control system to the automatic pilot. The present tie-in was developed under Navy contract by the McDonnell Aircraft Corporation. This tie-in essentially takes inputs of radar-tracking line position, computed lead angle, and various airplane response parameters and computes control-deflection commands for the aileron and elevator channels of the autopilot. The rudder channel of the autopilot was not connected to the tie-in and was used solely for yaw damping. The major components of the tie-in, located in a well in the left wing, are shown in the photograph in figure 3.

The autopilot used was also a component of the production version of the airplane, its original purpose being to function as a relief autopilot. The control loops of the autopilot were modified somewhat for use in the automatic system; however, the original low-torque parallel-installed servos were retained. Some data on the performance of the autopilot servos are included in reference 5.

During the tests discussed herein the computed lead-angle inputs were eliminated from the system. Without lead-angle inputs the system attempted to fly pure pursuit trajectories (guns always aimed directly at the target). This modification was made in order to use photographic data from a fixed gun sight to study the performance of the system. As would be expected, elimination of the computer provided more favorable input characteristics to the tie-in than existed with the computer operating. In particular, the computer was eliminated as a source of noise; however, preliminary tests with the computer in and with the computer out indicated no particular effect on optimum parameter settings of the system in tail chase or steady turns.

Elevation Channel

A block diagram showing the elevation channel of the automatic interceptor system is shown in figure 4(a). A potentiometer mounted on the radar-antenna elevation gimbal is used to measure the elevation gun-line error. This signal in effect commands a rate of pitch of the airplane as indicated by the pitch rate feedback in the diagram. In order to aid in stabilizing the pitch-rate loop the signal from the rate gyro was electrically differentiated and this angular acceleration signal also was fed back to the tie-in. This combined signal provides the elevation-deflection command to the autopilot servo loop. The autopilot servomotor directly actuates the power-control system of the airplane and works against the feel-system loads. The feel system essentially is the same as in the production airplane (see ref. 6); however, a bungee which provided a stable stick-force variation with speed is eliminated. The elevator-deflection command is modified by a lag-lead network in the tie-in in order to provide lead at high frequencies and thereby compensate in part for the servo lag. Details of the various tie-in networks and the gain constants used are presented in reference 5.

Deflection Channel

A block diagram showing the deflection channel of the automatic interceptor system is shown in figure 4(b). In this case the tracking-line error (approximately the gun-line error) plus the integral of the tracking-line error command a proportional bank angle. In a steady turning maneuver where a steady bank angle is being maintained, a signal

proportional to bank angle is continuously fed into the tie-in. Without the error integral signal a steady tracking error would be required to generate a signal canceling the bank-angle signal and thereby maintain a steady bank angle. In order to eliminate this steady-state tracking error the integral signal is used to cancel the bank-angle feedback.

In addition to the feedback of bank angle, negative feedbacks of roll rate and roll acceleration are provided to stabilize the control loop. The combined signal provides the aileron-deflection commands to the autopilot servomotor and, as in the case of the elevation channel, the servomotor directly actuates the power-control system of the airplane and operates against the feel-system loads (which are the same as for the production airplane). A lag network is included in the bank-angle feedback circuit to the tie-in in order to attenuate the signal at high frequencies and thereby improve the stability of the control loop.

FLIGHT-TEST PROCEDURES

All flight tests were conducted by using a cooperative jet aircraft as a target. A series of attack situations and target maneuvers were designed to provide inputs to the automatic interceptor system representative of those that might occur during an actual attack. At the same time the runs were simplified to afford reasonable ease in setting up the initial conditions for a given run and to maintain reasonable repeatability of a given situation or maneuver.

The tracking performance was studied under the following basic conditions:

(1) Steady tracking of a nonmaneuvering target with the interceptor in tail-chase position

(2) Steady tracking during a constant-acceleration turn by the target

(3) Tracking during abrupt turn entries following steady tracking in the tail-chase position

(4) Tracking during abrupt push-downs and pull-ups following steady tracking from tail-chase position

(5) Engagement of the system from tail-chase position with a nonmaneuvering target but with an initial gun-line error in elevation or in azimuth

All runs were made at an initial altitude of 20,000 feet and at a Mach number of about 0.76. Most runs were made with the system engagement at 1,000-yards range and no initial closing rate. No provision existed in the system for automatic gain variations with flight conditions, and the foregoing flight condition was the one for which the best gain settings for the basic system had been established. Except where variations in specific system parameters were studied, the gain settings were those recommended in reference 5.

Method of Analysis

After preliminary testing indicated that comparatively long times were required by the original system to reduce deflection errors during target turn entries, it was decided to conduct an analysis to compare the original system (with and without error integration) to other systems having alternate means for eliminating steady-state errors. Since the purpose of the analysis was to determine qualitatively the effect of certain system modifications rather than to obtain detailed correlation with flight results, it was decided to make a simplified linear analysis using Laplace transformations, and no particular effort was made to simulate detailed dynamics of components of the test system. From this study it was hoped to gain more insight into the fundamental nature of the problem than might have been possible in a very complex simulation.

The responses of the basic and alternate deflection systems related to three operational situations were investigated. The first situation was an abrupt entry into a turn by the target, the second was the engagement of the system with an existing steering error, and the third was a sinusoidal maneuver by the target.

The development of equations describing the response of the three systems and a more complete description of the assumed systems has been set apart in appendix A.

Description of Alternate Means for Eliminating Steady-State Errors

The two alternate systems included in this analysis were designed to improve the response of the deflection channel to target turns. Both utilize the principle of differentiation to provide anticipation of target maneuvers.

System with error differentiation.- The first of these alternate systems, referred to as the system with error differentiation, utilizes a differentiated error signal to stabilize the tracking loop rather

than by use of the feedback of bank angle. Thus, by eliminating bank-angle feedback the source of steady-state errors in turns is eliminated and the need for error integration is eliminated. It was recognized that any system using error differentiation might not be practical because of deleterious effects of the error differentiation on the system response to radar noise. Appendix B presents additional information on this subject. Still, a comparison on a noise-free basis of such a system with one having error integration appeared worthwhile in that some idea would be gained as to the penalities involved in using bank-angle feedback for stabilization with the associated need for integration.

System with input differentiation.- The second of the alternate systems, referred to as the system with input differentiation, was designed to maintain the essential feature of the system with error differentiation but to alleviate as much as possible the noise problem. This system retains the bank-angle feedback of the basic system but instead of using error integration to generate a signal canceling the bank-angle feedback a signal is used that is proportional to the radar antenna rate in deflection. When the interceptor tracks a target in a steady turn this antenna deflection-rate signal is approximately proportional to the bank angle. This signal is obtained from the deflection antenna-rate gyro and filtered to remove noise signals at frequencies higher than those associated with target maneuvers. The signal is then fed forward to be summed with the error signal at the tie-in. The antenna-rate signal provides the feature of anticipation of target turning maneuvers and, since the source of the canceling signal is outside the tracking loop, the feature of the canceling signal not affecting the stability of the interceptor tracking loop.

Modifications for flight test of system with input differentiation.- The results of the analytical studies indicated that the system with filtered input differentiation had better tracking performance than the basic system. Therefore, it was desirable to flight test the system with filtered input differentiation.

A modification to the basic system to provide the desired system (see fig. 5) was quite simply made by eliminating the error integral signal from the tie-in and by using the deflection-lead-angle servo of the fire-control computer to provide the filtered input rate signal. In the normal computation of lead angle the antenna rate is multiplied by a computed projectile time of flight. For this modification the time-of-flight servo was locked in a position to provide the desired sensitivity between antenna rate and signal to the tie-in. Additional amplification was required to obtain this sensitivity, and this increased the noise emanating from the computer.

No modification in the response of the computer was made and the overall filtering in the computer corresponded to a time constant (relating tie-in input to antenna rate) of 1.4 seconds. It might be pointed out that although the computer was not used to compute lead angle

in the flight tests, the error correction and lead-angle computation could easily be done simultaneously. The correction would be obtained simply by adding a voltage to the output of the time of flight potentiometer. This arrangement would operate satisfactorily up to moderate bank and pitch angles since in this range the space rate of the antenna is a measure of bank angle. In order to obtain satisfactory operation for large values of bank and pitch angles, additional corrections can be applied. If yaw feedback could be used in place of bank-angle feedback to stabilize the deflection tracking loop, the need for this additional correction factor could perhaps be eliminated, but this arrangement was not investigated.

RESULTS AND DISCUSSION

Flight Tests of Basic Interceptor System

General.- The response of the original interceptor system was investigated under the basic conditions listed in the section entitled "Flight-Test Procedures." Typical time histories of gun-line errors obtained from each run are presented in figures 6 to 11.

Figure 6 shows part of a typical time history of tracking error obtained during steady tracking of a nonmaneuvering target with the interceptor in tail-chase position. In the analysis of these data the gun-line wander was referenced to the approximate center-of-gravity position of the target. The standard deviations of tracking errors were determined from considerably more tracking than shown in figure 6. From about 90 seconds of tracking the standard deviations were found to be 2.6 mils in deflection and 2.2 mils in elevation. This is considered to be good tracking, and the standard deviation values are comparable to those obtained with human-pilot tracking using an optical sight (ref. 7) and is somewhat better than obtained with a human pilot using a radar fire-control system and radarscope display.

Response characteristics of elevation channel.- The ability of the elevation channel to reduce an engagement error (53 mils) is shown by the time history presented in figure 7. The initial response is rapid, but the first overshoot is large (46 mils); however, the system then settles to steady tracking and small errors (less than 5 mils) in about 5 seconds from engagement. The settling time of the elevation channel appears adequate for present-day intercept operations and compares favorably with times involved when human-pilot control is used.

The response of the elevation channel to push-down and pull-up maneuvers by the target was, in general, fairly good although no provision was made to eliminate steady maneuvering errors. The magnitude

of these steady-state errors was not readily obtainable from the flight tests since steady normal acceleration was maintained only for brief intervals during push-down and pull-up maneuvers and the values determined from flight-test runs involving steady turning maneuvers were inconsistent due to inconsistent variations of elevation error. Considerations of the gains employed in the elevation channel indicated this steady-state error would be about 15 mils/g.

Response characteristics of deflection channel.- The ability of the deflection channel to reduce a lateral engagement error of 60 mils is shown by the time history presented in figure 8. The apparent lag in initiation of a correction of the error after engagement is due to the fact that the gun line was depressed below the axis about which the interceptor rolled. Thus, rolling of the interceptor under this condition actually tends to force the gun line away from the target. Additional records of aileron angle, roll rate, and bank angle showed that the ailerons were deflected and that the airplane began to roll immediately on engagement.

After this apparent lag the lateral error was rapidly reduced but an initial overshoot of 26 mils occurred. The subsequent response was slow and somewhat oscillatory, with the result that the gun-line error was still about 7 mils at 20 seconds from engagement (at which time the target rolled into a moderate horizontal turn).

The time history presented as figure 9 shows the variation in gun-line error during this turning maneuver. The gun-line error peaked at over 40 mils about 9 seconds after the initiation of the target turn. The error was then reduced slowly and did not reduce below 5 mils until almost 20 seconds after the start of the maneuver. Once the transient error was reduced, the deflection errors were maintained at about as low a level in the steady turn as in a tail chase on a nonmaneuvering target. Because of the long settling times involved, however, it is obvious that by undergoing mild continuous lateral evasion the target could have maintained large gun-line errors practically the entire time.

Effect of gain variation on performance of deflection channel.- Two direct possibilities for improvement in the performance of the system are to increase the ratio of bank angle to deflection error and to increase the gain on the error integral signal. The former could be accomplished by either an increase in gain on the steering-error signal or by a decrease in the gain on the bank-angle signal. As shown in figure 10, however, the stability of the tracking loop was so deleteriously affected by such gain adjustments that this means of reducing the steady-state errors of the deflection system was precluded. Attempts to utilize higher forward-loop gains by increasing the gains of the feedback signals in the inner loop were not successful because of the occurrence of high-frequency lightly-damped oscillations when such increases were attempted.

The second possibility, increasing the gain on the integral signal, was also investigated in flight and the results are presented as time histories in figure 11. Time histories of the transient gun-line errors following a target turn are presented in figure 11(a) for three values of integrator gain.

The case with zero gain on the integral signal is of interest to establish the magnitude of the bias errors which had to be compensated by the integrator. As shown in the figure, the bias is about 145 mils for the example turn which resulted from a steady bank angle of 30°. The use of an integral signal with a normal gain setting serves to eliminate ultimately this bias error; but, as discussed previously, the peak of the transient error and the time required for this error to settle to low values are excessive. The run with the increased integrator gain in figure 11(a) was made with the gain set at close to the highest value available in the system (about 2 times the normal setting). With this higher setting the transient error following a target turn was significantly reduced both as to peak error and the time to reduce this error; however, the error and settling time are still much larger than desirable and indicate that further increases in the gain on the integral signal were needed. Practically, the ability to utilize still higher gains is negated by effects on tracking-loop stability. Tracking-loop oscillations are not greatly excited by a target turning maneuver of the type shown, but the effect of integrator gain on the damping of these oscillations can be seen from the results presented in figure 11(b) where time histories of responses to engagement errors are shown. The oscillations are excited much more with this type of input and actually might be excited even more by rough air or by encountering the wake of target.

Analytical Results

Response to an abrupt turn by the target and to an engagement with an initial error.- For comparison of the error response of the three systems studied to inputs approximating a target turn maneuver and an engagement with an initial error, the inverse transforms were taken of equations (A13), (A14), (A15), (A16), (A17), and (A18) to obtain equations of the time response. This operation was done by conventional procedures. (See ref. 8.)

For the basic deflection system, time histories of the computed responses to approximations of a target turning maneuver and an engagement with an initial error are presented in figure 12. Responses are shown for cases where the ratios of integrator gain to steering-error gain were 0.2, 1.0, and 0. The 0.2 case was considered to be the normal gain.

As mentioned previously, the analysis was applied to a much-simplified representation of the actual interceptor system. It may be seen that this analysis of the simplified system qualitatively predicts the same response characteristics obtained during flight tests by comparing corresponding curves of figure 12 with those of figure 11. Qualitative agreement exists as to the large steady-state error encountered in a turning maneuver when no integration is used, as to the large transient peak and long settling times in countering a turning maneuver when normal integration is used, and as to the detrimental effect on system stability indicated by the response to an engagement error when increased integrator gain is used.

The response of the system with error differentiation to a target turn (fig. 13) shows a very marked improvement over the system where integration was used for elimination of the steady-state error (the response of the basic system is also shown in the figure for comparison). For the error-differentiation system the gun-line error never exceeds 5 mils while countering a target turn. The oscillation apparent in the response is associated with the airplane-autopilot loop. Although studies of equations (A13) and (A14) show that the frequency and damping of this mode are little different for the basic system as compared with the error-differentiation system, the oscillation is excited more for the latter system primarily because of the differentiation of the input signal. This input differentiation provides a favorable anticipatory effect with respect to improving the response to target maneuvers.

The response of the system to an engagement error is fairly rapid with no overshoot. This response is the same as would be obtained with the basic system if no integral signal was present. This result occurs because the two systems have the same characteristic equation and the simplified analysis neglects the input due to interceptor lateral translation (a small effect for the ranges considered herein).

The system with filtered input differentiation is aimed at approximating the desirable response associated with the error-differentiation system yet affording a practical system design from the noise considerations. Time histories of the responses to a target turn and to an engagement error are also presented in figure 13. The response to a target turn of the system with filtered input differentiation is intermediate of the other two systems. The peak error is under 20 mils and the time to reduce to 5 mils is about 10 seconds from the start of the maneuver.

The filter time constant chosen for the analysis was 1 second. For smaller values of time constant the response of the system with filtered input differentiation to a target turn would approach that of the system with error differentiation, whereas for larger values of the filter time constant the response would approach that for the basic system without error integration.

By neglecting the minor effect of interceptor lateral translation the response of the system with filtered input differentiation to an engagement error is the same as the system with error differentiation and is the same as the basic system without error integration.

Response to a sinusoidal maneuver by the target.- The ability of an automatic interceptor system to counter evasive maneuvers by a target is likely to be a function of the characteristics of the evasive maneuver. It is conceivable that a target could take advantage of any characteristic of the response of the interceptor (sharp resonances) that would lead to a poorer tracking performance. The possibility that such characteristics exist in a given system can be explored by determining the frequency-response relationship of interceptor tracking error to target accelerations, and for this reason it was desirable to determine such relationships for the interceptor systems considered in this paper. The transfer functions relating tracking error and target lateral acceleration for the three deflection systems studied have been developed in appendix A. In order to compare the frequency response of these three systems, $i\omega$ was substituted for p in equations (A24), (A27), and (A31).

Frequency-response data for the basic deflection system with error integration and for the modified deflection system with filtered input differentiation are presented in figure 14. This figure includes the effect of varying the integrator gain and the filter time constant of the respective systems. The special cases of zero integrator gain and zero filter time constant are included.

As shown in figure 14 the amplitude ratio of tracking error in mils to target acceleration in g units for the case of zero integrator gain shows that a peak of about 130 mils/g occurs at a frequency of about 0.2 radian/second. With the integrator gain set at the value considered normal for the assumed system, $K_I/K_\sigma = 0.2$, there was an increase in the magnitude of the amplitude-ratio peak to about 145 and a slight increase in the peak frequency (to about 0.3 radian/sec). The major change due to the finite integration is to cause the amplitude ratio to go to zero at zero frequency. This characteristic reflects the ability of the integrator to eliminate errors occurring over long periods; however, by discrete choice of maneuver the target can still generate peak errors of the same magnitude as the system without error integration. The curves representing the increased integrator gain K_I/K_σ show an increase in the amplitude-ratio-peak magnitude (to about 210) and frequency (to about 0.7 radian/sec). Delaying the amplitude-ratio rise to higher frequencies reflects the ability of the integrator to eliminate steady errors more rapidly; however, the increase in the magnitude of the peak indicates that by discrete choice of frequency, the target can generate larger errors than occur without the integrator. As was noted in the section entitled "Effect of Gain Variation on Performance of Deflection Channel," the ability to utilize high integrator gains is limited by a

practical consideration of the effect on tracking-loop stability. This limitation on the integrator gain is borne out by the fact that further increases in integrator gain caused the amplitude ratio to peak at extremely high magnitudes. A target airplane would be capable of generating lateral-acceleration oscillations of sufficient magnitude at frequencies in the region (0.2 to 0.7 radian/sec) of the amplitude-ratio peaks to create large interceptor tracking errors. It is believed that this deficiency would be common to interceptor systems characterized by low forward-loop gains and utilizing error integration for bias elimination.

Amplitude-ratio data are also presented for the system with error differentiation and the system with filtered input differentiation in figure 14. The curve representing the case where the filter time constant τ_f is zero is identical to that representing the system with error differentiation. If such a system could be used, the low-frequency resonances would be avoided and the errors generated by sinusoidal maneuvers could be maintained at low values regardless of frequency. As mentioned previously, this system would be impractical because of noise considerations. With a value of filter time constant of 1 second the peak error is about 20 mils/g, or less than 15 percent of that of the basic system with a normal integrator gain. The frequency at which the peak amplitude ratio occurs is again within the capabilities of an evading target, but by virtue of the large decrease in magnitude of the amplitude ratio the system tracking performance would be less susceptible to lateral oscillations by a target.

Flight Tests of Systems With Filtered Input Differentiation

Tracking performance.- The response characteristics of the modified system are illustrated in figure 15. Responses to an engagement error and to a target turn are presented; in addition, corresponding curves for the basic system with integration are shown for comparison. The initial response to an engagement error is about the same as for the basic system, but the overshooting characteristic and long settling time associated with the basic system are avoided.

The response to a target turn was much improved over the basic system in terms of the peak transient error and the time to reduce the error to small values. The peak error for the modified system was held to about 15 mils, and the error was reduced to 5 mils in about 5 seconds. These values are typical of those obtained for all the runs made with the modified system.

The tracking of the modified system in a steady tail chase is somewhat poorer than that obtained with the basic system because of the increased noise input to the tie-in. It is interesting that the tracking during the steady portion of turn was better than occurred in tail chase.

The standard deviation of tracking error obtained from three tail-chase runs comprising 80 seconds of record was 4.5 mils, whereas the standard deviation obtained from seven turns comprising 200 seconds of record was 3.5 mils. The cause of this result was traced to dead-spot oscillations of the multiplying servo in the computer which multiplied spacial antenna rates by a calibration factor to provide error-correction signals. This oscillation was more severe at zero correction (zero bank angle) than at values greater than zero (in turning flight). Actually, it appeared that these dead-spot oscillations of the multiplying servo were more responsible for noise signals to the tie-in system than was the noise associated directly with antenna rate signal. The high gain in the computer tended to aggravate the effects of the dead-spot oscillations, but it is believed that the noise from this source could have been materially reduced by reworking the multiplying servo. In spite of this difficulty, the tracking performance of the modified system was reasonably satisfactory as indicated by the figures of standard deviation of tracking error quoted heretofore.

Other considerations.- The use of this method for eliminating steady-state errors would be more applicable to systems affording higher forward-loops gains wherein the steady-state errors would be of the same order of magnitude as the kinematic lead angle rather than five times as large as occurred herein. The general idea of open-loop computation of steady-state errors also would appear useful in other applications such as the correction of the steady-state errors occurring in the elevation channel of the system. Another possible application such as described in reference 8 would be in a manual system wherein the pilot derives information from a radarscope display.

In the course of the flight tests, difficulty was experienced in maintaining the correct sensitivity between azimuth antenna rate and the corresponding voltage to the tie-in. This difficulty could perhaps be alleviated in a refined design, particularly as regards to close control of the temperature of components. This problem, however, is no different from that which occurs for the basic lead-angle computer and must be circumvented in order to obtain a practical system. In the case of the error computation some of the difficulty with sensitivity changes could perhaps be overcome by retaining a low-gain error integral signal in the loop.

CONCLUSIONS

In the foregoing investigation the tracking performance of an automatic interceptor system was studied and particular attention was devoted to the subject of steady-state-error elimination. Two alternate systems were included in the analytical phase of the studies, and one of these

alternate systems was mechanized in the automatic interceptor system and flight tested. As a result, the following conclusions are drawn:

1. The basic automatic interceptor system exhibited the following characteristics during flight tests:

(a) The tracking performance in a tail chase was good, the standard deviations of tracking error being 2.6 mils in deflection and 2.2 mils in elevation.

(b) The elevation tracking in response to an engagement error of 60 mils showed a large initial overshoot but settled rapidly to small error values (below 5 mils in about 5 seconds). The response of the elevation channel to steady push-down pull-up maneuvers by the target was considered fairly good although moderate bias errors were encountered.

(c) The deflection tracking in response to an engagement error of 60 mils at engagement overshot moderately and took about 20 seconds to reduce below 5 mils. The response to mild target turns showed large peak errors (40 to 60 mils) and long settling times (20 seconds) following the turn entry. These large peak errors and long settling times are associated with a large correction being required and the correction being supplied by a relatively low gain-error integrator.

2. Increasing the forward-loop gain of the deflection channel and increasing the deflection-channel integral gain to improve the interceptor deflection-tracking performance adversely affected the stability of the tracking loop.

3. Comparisons by means of a simplified analytical study of the basic system with error integration with two alternate deflection systems specifically designed for steady-state-error elimination showed the following results:

(a) A system using error differentiation to stabilize the tracking loop eliminates the source of the steady-state error. While not practical from a radar-noise standpoint, such a system is capable of much improved tracking performance in countering target turns with a noise-free system.

(b) A system using filtered input differentiation for an open-loop computation of the bias-error correction appears practical from a radar-noise standpoint and is capable of an improved performance over the basic system with error integration.

4. A frequency-response analysis indicated that the basic deflection channel with error integration would have very large tracking errors in attempting to counter a target undergoing sinusoidal lateral-acceleration oscillations at some discrete frequency between 0.2 and 0.7 radian/second

because of sharp system resonances. The situation could not be improved by adjustment of the gain on the integral signal. The filtered-input-differentiation system had a peak error which was less than 15 percent of the peak error of the basic system with integration.

5. Flight-test results using the principle of filtered input differentiation in the deflection channel showed the following results as compared to the basic deflection system:

(a) The settling time following an engagement with an initial deflection error was reduced while the initial rapid response was maintained.

(b) The peak deflection error following a target turn entry was reduced from 40 to 60 mils to about 15 mils.

(c) The transition time following a target turn entry was reduced from about 20 seconds to about 5 seconds.

(d) The tail-chase tracking was somewhat poorer but the values of tracking-error standard deviation were fairly low (4.5 mils). The poorer tracking characteristics of the filtered-input-differentiation system during tail-chase tracking were traced in part to computer dead-spot oscillations which apparently contributed more to the total noise signal than the antenna rate signals.

6. The principle utilized in the filtered-input-differentiation system should be applicable to other types of automatic systems and should give more favorable results if these systems afford the use of higher gains than were possible in the present automatic interceptor system.

7. The flight tests of the filtered-input-differentiation system indicated problems of calibration stabilization of the open-loop computer elements. These problems require consideration in a practical application of the filtered-input-differentiation principle.

Langley Aeronautical Laboratory,
National Advisory Committee for Aeronautics,
Langley Field, Va., April 16, 1956.

APPENDIX A

DEVELOPMENT OF EQUATIONS PERTAINING TO RESPONSE OF AUTOMATIC-INTERCEPTOR-DEFLECTION SYSTEM TO INPUTS APPROXIMATING VARIOUS OPERATIONAL SITUATIONS

GENERAL

The purpose of this appendix is to develop equations pertaining to the response of simplified linear versions of three automatic-interceptor deflection systems to inputs approximating three operational situations. These situations include (1) an abrupt entry into a steady turn by the target, (2) engaging the system with an existing steering error, and (3) a sinusoidal maneuver by the target. Since in the latter case it was desirable to use a more exact representation of problem geometry, this situation will be considered separate from the first two.

The dynamics of the radar tracking system were not considered because comparison of flight records of radar-tracking-line position and gun-line position (obtained by gun-sight aiming-point camera records) showed that the radar tracking during maneuvers and steady conditions was fairly good and could not account for the large transient errors observed during turn entries. Although the radar dynamics were eliminated from the analysis, consideration was given to the probable effects of radar noise on the system modifications which were considered.

Another simplification was the assumption that the roll-rate response of the airplane to commands (when equalized by the roll acceleration and roll-rate autopilot loops) could be represented by a linear lag. In addition, no modifying networks such as existed in the feedback of bank angle in the flight-test system were included.

RESPONSE TO AN ABRUPT TURN BY THE TARGET AND TO AN ENGAGEMENT WITH AN INITIAL ERROR

Discussion of Inputs

The first situation studied was the interceptor response to an abrupt turn by the target. This situation was approximated by applying a step

in $\dot{\psi}_i$. As shown in appendix B of reference 10, for pursuit attacks constant value of $\dot{\psi}_i$ would be approached if the target maintained constant acceleration in a turn. There is, however, a linear lag (with a time constant equal to the range divided by the target speed) in the approach to the steady value even if the target could apply its acceleration instantly. The lag would be increased further by the time required for the target to build up the acceleration. Use of a step in $\dot{\psi}_i$ was justified, however, on the basis that it was a more taxing input than an actual turn entry. It also was felt that an actual turn entry would be fairly well approximated simply by considering the target maneuver to be initiated a number of seconds earlier than the time when the step in $\dot{\psi}_i$ was applied.

The second situation studied was the response of the system following its engagement with the radar already locked on the target but with a steering error existing at engagement. This case was approximated by assuming zero input with an initial conditon on σ. The approximation neglects the space rate of the line of sight generated by the lateral translation of the interceptor and assumes that there is no other coupling between the radar tracking line and the motions of the interceptor.

Development of System Equations

Basic system with error integration.- A block diagram of the simplified version of the basic deflection system which employs error integration to correct steady-state errors is presented in figure 16(a). For this system, the following equations apply:

$$\dot{\sigma} = \dot{\psi}_i - \dot{\psi}_o \tag{A1}$$

$$\epsilon_1 = K_\sigma \sigma + K_I \int_0^t \sigma \, dt \tag{A2}$$

$$\epsilon_2 = \epsilon_1 - K_\phi \phi \tag{A3}$$

$$K_{\dot{\phi}} \tau_a \ddot{\phi} + K_{\dot{\phi}} \dot{\phi} = \epsilon_2 \tag{A4}$$

$$\dot{\psi}_o = \frac{g}{V} \phi \tag{A5}$$

Transforming to the Laplace domain gives

$$p\sigma(p) - \sigma_{(o)} = \dot{\psi}_i(p) - \dot{\psi}_o(p)$$

$$\epsilon_1(p) = K_\sigma\sigma(p) + K_I \frac{\sigma(p)}{p}$$

$$\epsilon_2(p) = \epsilon_1(p) - K_\phi\phi(p)$$

$$K_{\dot{\phi}}\tau_a p^2\phi(p) - K_{\dot{\phi}}\tau_a p\phi_{(o)} - K_{\dot{\phi}}\tau_a\phi_{(o)} + K_{\dot{\phi}}p\phi(p) - K_{\dot{\phi}}\phi_{(o)} = \epsilon_2(p)$$

$$\dot{\psi}_o(p) = \frac{g}{V}\phi(p)$$

Solving for $\sigma(p)$ as a function of $\dot{\psi}_i(p)$ gives

$$\sigma(p) = \frac{\left(p^2 + \frac{1}{\tau_a}p + \frac{1}{\tau_a}\frac{K_\phi}{K_{\dot{\phi}}}\right)\left[\dot{\psi}_i(p) + \sigma_{(o)}\right] + \frac{g}{V}\left[\left(p + \frac{1}{\tau_a}\right)\phi_{(o)} + \dot{\phi}_{(o)}\right]}{p^3 + \frac{1}{\tau_a}p^2 + \frac{1}{\tau_a}\frac{K_\phi}{K_{\dot{\phi}}}p + \frac{g}{V}\frac{1}{\tau_a}\frac{K_\sigma}{K_{\dot{\phi}}} + \frac{g}{V}\frac{1}{\tau_a}\frac{K_I}{K_{\dot{\phi}}}\frac{1}{p}} \quad \text{(A6)}$$

The system parameters τ_a and $K_\phi/K_{\dot{\phi}}$ were adjusted so that the natural frequency of the roll-attitude loop (as determined from equations (A3) and (A4)) was one-half cycle per second and so that oscillations generated within the loop damped to one-quarter amplitude in one cycle. The forward-loop gain was adjusted to command 10° of bank angle for each degree of steering error and the integral gain was made one-fifth the proportional gain. These gain adjustments resulted in a damping ratio of 0.7 for the long-period oscillatory mode of the system. The frequency of this oscillation was about 1 radian per second, and the break frequency due to integration was about 2 octaves below the natural frequency of the long-period mode.

System with error differentiation.- For the system with error differentiation, which is presented in figure 16(b), equations (A1), (A4), and (A5) still apply, and in addition the following equation applies

$$\epsilon_2 = K_\sigma\sigma + K_D\dot{\sigma} \quad \text{(A7)}$$

The Laplace transform of this equation is

$$\epsilon_2(p) = K_\sigma\sigma(p) + K_D p\sigma(p) - K_D\sigma_{(o)}$$

Solving the transformed form of equations (A1), (A4), (A5), and (A7) for $\sigma(p)$ as a function of $\psi_i(p)$ gives

$$\sigma(p) = \frac{p\left(p + \frac{1}{\tau_a}\right)\dot{\psi}_i(p) + \left(p^2 + \frac{1}{\tau_a} p + \frac{1}{\tau_a} \frac{g}{V} \frac{K_D}{K_{\ddot{\phi}}}\right)\sigma_{(o)} + \frac{g}{V}\left[\left(p + \frac{1}{\tau_a}\right)\phi_{(o)} + \dot{\phi}_{(o)}\right]}{p^3 + \frac{1}{\tau_a} p^2 + \frac{1}{\tau_a} \frac{g}{V} \frac{K_D}{K_{\ddot{\phi}}} p + \frac{1}{\tau_a} \frac{g}{V} \frac{K_\sigma}{K_{\ddot{\phi}}}} \tag{A8}$$

The error-differentiation gain was adjusted to provide the same coefficient for the p term of the characteristic equation as existed for the basic system; that is,

$$\left.\frac{K_D}{K_{\ddot{\phi}}}\right|_{\text{error differentiation}} = \left.\frac{V}{g} \frac{K_\phi}{K_{\ddot{\phi}}}\right|_{\text{basic system}}$$

In this way the characteristic equation of the system with error differentiation is the same as the basic system without error integration and the response to an engaging error is the same for the system with error differentiation as for the basic system without error integration.

System with filtered input differentiation.- For the system with filtered input differentiation, which is presented in figure 16(c), equations (A1), (A3), (A4), and (A5) for the basic system still apply and the relation for ϵ_1 is

$$\epsilon_1 = K_\sigma \sigma + K_D \bar{\dot{\psi}}_i \tag{A9}$$

where

$$\bar{\dot{\psi}}_i = \dot{\psi}_i - \tau_f \frac{d\bar{\dot{\psi}}}{dt} \tag{A10}$$

Assuming no initial conditions of $\bar{\dot{\psi}}_i$ (if filtering is provided by an RC filter, for example, then no initial charge is assumed to exist on the condenser), the Laplace transform of equation (A10) is

$$\bar{\dot{\psi}}_i(p) = \dot{\psi}_i(p) - p\bar{\psi}_i(p)$$

Solving for $\bar{\dot{\psi}}(p)$ and substituting into the transformed form of equation (A9) gives

$$\epsilon_1(p) = K_\sigma \sigma(p) + K_D \frac{\psi_i(p)}{1 + \tau_f p} \tag{A11}$$

Solving the transformed form of equations (A1), (A3), (A4), and (A5) together with equation (A11) for $\sigma(p)$ as a function of $\dot{\psi}_i(p)$ gives

$$\sigma(p) = \frac{\left[p^2 + \frac{1}{\tau_a} p - \frac{g}{V} \frac{1}{\tau_a} \frac{K_D}{K_{\dot{\phi}}} \left(\frac{1}{1 + \tau_f p}\right) + \frac{1}{\tau_a} \frac{K_\phi}{K_{\dot{\phi}}}\right] \dot{\psi}_i(p) + \left(p^2 + \frac{1}{\tau_a} p + \frac{1}{\tau_a} \frac{K_\phi}{K_{\dot{\phi}}}\right) \sigma(o) + \frac{g}{V} \left[\left(p + \frac{1}{\tau_a}\right) \phi(o) + \dot{\phi}(o)\right]}{p^3 + \frac{1}{\tau_a} p^2 + \frac{1}{\tau_a} \frac{K_\phi}{K_{\dot{\phi}}} p + \frac{g}{V} \frac{1}{\tau_a} \frac{K_\sigma}{K_{\dot{\phi}}}} \tag{A12}$$

RESPONSE TO TARGET TURNS

The Laplace representation of a step in $\dot{\psi}_i$ is $\dot{\psi}_i(p) = \frac{A}{p}$ where A is a constant equal to the magnitude of the step. Substituting this equation into equations (A6), (A8), and (A12) and assuming zero initial conditions gives for the basic system with error integration

$$\sigma(p) = \frac{A\left(p^2 + \frac{1}{\tau_a} p + \frac{1}{\tau_a} \frac{K_\phi}{K_{\dot{\phi}}}\right)}{p^4 + \frac{1}{\tau_a} p^3 + \frac{1}{\tau_a} \frac{K_\phi}{K_{\dot{\phi}}} p^2 + \frac{1}{\tau_a} \frac{g}{V} \frac{K_\sigma}{K_{\dot{\phi}}} p + \frac{1}{\tau_a} \frac{g}{V} \frac{K_I}{K_{\dot{\phi}}}} \tag{A13}$$

for the system with error differentiation

$$\sigma(p) = \frac{A\left(p + \frac{1}{\tau_a}\right)}{p^3 + \frac{p^2}{\tau_a} + \frac{1}{\tau_a} \frac{g}{V} \frac{K_D}{K_{\dot{\phi}}} p + \frac{1}{\tau_a} \frac{g}{V} \frac{K_\sigma}{K_{\dot{\phi}}}} \tag{A14}$$

and for the system with filtered input differentiation

$$\sigma(p) = \frac{A\left[p^2 + \frac{1}{\tau_a} p - \frac{g}{V} \frac{1}{\tau_a} \frac{K_D}{K_{\dot{\phi}}} \left(\frac{1}{1 + \tau_f p}\right) + \frac{1}{\tau_a} \frac{K_\phi}{K_{\dot{\phi}}}\right]}{p\left(p^3 + \frac{1}{\tau_a} p^2 + \frac{1}{\tau_a} \frac{K_\phi}{K_{\dot{\phi}}} p + \frac{g}{V} \frac{1}{\tau_a} \frac{K_\sigma}{K_{\dot{\phi}}}\right)} \tag{A15}$$

A comparison of equation (A15) with equation (A14) shows that for the input approximating a turning maneuver the system with filtered input differentiation approaches the behavior of the system with error differentiation at values of $\tau_f p$ which are small compared to unity (low frequencies) provided that K_D is adjusted to equal $\frac{V}{g} K_\phi$. At large values of $\tau_f p$ (high frequencies) the system approaches the behavior of the basic system without error integration. (Compare eqs. (A15) and (A13).) The frequency range over which the behavior of the modified system approximates the basic system without error integration is determined by the value chosen for the filter time constant, and it would appear that the time constant would be dictated by the probable highest frequency of target maneuvers; however, because this time constant determines the cutoff frequency of the network which filters the tracking-line rate (the chief source of radar noise), the choice of this time constant must also be compatible with the requirement that the root-mean-square (rms) steering errors due to radar noise be maintained at a satisfactorily low level. A brief analysis of the radar-noise problem was made and is presented in appendix B. From this analysis it appeared that a filter-time constant of 1 second was a satisfactory compromise between the conflicting requirements of radar-noise attenuation and good response to target maneuvers.

RESPONSE FOLLOWING AN ENGAGEMENT WITH AN INITIAL ERROR

For the case where an engagement is made with an initial error $\left(\sigma_{(o)} = \text{finite value}\right)$ and the target does not maneuver $\left(\dot{\psi}_i(p) = 0\right)$, equations (A6), (A8), and (A12) become for the basic system with error integration

$$\sigma(p) = \frac{\sigma_{(o)} p\left(p^2 + \frac{1}{\tau_a} p + \frac{1}{\tau_a} \frac{K_\phi}{K_{\dot{\phi}}}\right)}{p^4 + \frac{1}{\tau_a} p^3 + \frac{1}{\tau_a} \frac{K_\phi}{K_{\dot{\phi}}} p^2 + \frac{1}{\tau_a} \frac{g}{V} \frac{K_\sigma}{K_{\dot{\phi}}} p + \frac{1}{\tau_a} \frac{g}{V} \frac{K_I}{K_{\dot{\phi}}}} \tag{A16}$$

for the system with error differentiation

$$\sigma(p) = \frac{\sigma_{(o)}\left(p^2 + \frac{1}{\tau_a} p + \frac{1}{\tau_a} \frac{g}{V} \frac{K_D}{K_{\dot{\phi}}}\right)}{p^3 + \frac{1}{\tau_a} p^2 + \frac{1}{\tau_a} \frac{g}{V} \frac{K_D}{K_{\dot{\phi}}} p + \frac{1}{\tau_a} \frac{g}{V} \frac{K_\sigma}{K_{\dot{\phi}}}} \tag{A17}$$

for the system with filtered input differentiation

$$\sigma(p) = \frac{\sigma_{(o)}\left(p^2 + \frac{1}{\tau_a} p + \frac{1}{\tau_a} \frac{K_\phi}{K_{\dot{\phi}}}\right)}{p^3 + \frac{1}{\tau_a} p^2 + \frac{1}{\tau_a} \frac{K_\phi}{K_{\dot{\phi}}} p + \frac{1}{\tau_a} \frac{g}{V} \frac{K_\sigma}{K_{\dot{\phi}}}} \tag{A18}$$

A comparison of equation (A18) with equation (A16) shows that the response to an engagement error for the system with filtered input differentiation is the same as for the basic system without error integration. Provided that the gain K_ϕ of the system with filtered input differentiation is made equal to $\frac{V}{g} K_D$ of the system with error differentiation (the relation always used herein), comparing equation (A18) and equation (A17) shows that the response of these two systems to an engaging transient also will be the same.

RESPONSE TO A SINUSOIDAL MANEUVER BY THE TARGET

Basis of Analysis and Assumptions

The response of the interceptor to a sinusoidal maneuver by the target would consist of a transient portion followed by a steady-state portion (provided the response of the system is stable). In this case the steady-state portion is of primary interest and since initial conditions do not affect this portion of the response they will be omitted. The steady-state response of a system to a sinusoidal input may be described by frequency-response plots which relate the amplitude and phase of the system output to the input as a function of input frequency. (See ref. 1.)

In this analysis the assumption was made that the target performed oscillatory maneuvers in the horizontal plane. Although the target resultant acceleration was always in the horizontal plane, its time history was of such a form as to make the component (including gravity) in the plane of the interceptors wings always sinusoidal.

By assuming the interceptor does not sideslip its geometric lateral acceleration (in the plane of the wings) is, to a good degree of approximation, proportional to the interceptor bank angle. With the foregoing assumptions a linear analysis was afforded. The resulting block diagrams representing the three deflection systems considered in this paper are presented in figures 17(a), (b), and (c); these diagrams are essentially

the same as those presented in figures 16(a), (b), and (c) except for the differences in the input from the target and in the problem geometry. The equations involving the interceptor-target geometry which were used to determine the interceptor tracking error and special rate of the line of sight are presented in reference 10.

Development of System Transfer Functions

Basic system with error integration.- The assumed diagram for this system is shown in figure 17(a) and the following equations apply:

$$\sigma = \frac{1}{R}\int_0^t \int_0^t a_B \, dt^2 - \frac{1}{R}\int_0^t \int_0^t a_F \, dt^2 - \frac{1}{R}\int_0^t \frac{R}{V} a_F \, dt \qquad (A19)$$

$$\epsilon_1 = K_\sigma \sigma + K_I \int_0^t \sigma \, dt \qquad (A20)$$

$$a_F = Gg\phi \qquad (A21)$$

$$\epsilon_2 = \epsilon_1 - K_\phi \phi \qquad (A22)$$

$$\epsilon_2 = K_{\dot{\phi}} \tau_a \ddot{\phi} + K_{\dot{\phi}} \dot{\phi} \qquad (A23)$$

Transforming these equations into the Laplace domain and neglecting initial conditions gives

$$\sigma(p) = \frac{1}{R_p}\left[\frac{a_B(p)}{p} - a_F(p)\left(\frac{R}{V} + \frac{1}{p}\right)\right]$$

$$\epsilon_1(p) = K_\sigma \sigma(p) + \frac{K_I \sigma(p)}{p}$$

$$a_F(p) = Gg\phi(p)$$

$$\epsilon_2(p) = \epsilon_1(p) - K_\phi \phi(p)$$

$$K_{\ddot{\phi}} \tau_a p^2 \phi(p) + K_{\dot{\phi}} p \phi(p) = \epsilon_2(p)$$

Solving for the transfer function $\frac{\sigma(p)}{a_B(p)}$ gives

$$\frac{\sigma(p)}{a_B(p)} = \frac{p^3 + \frac{1}{\tau_a} p^2 + \frac{1}{\tau_a} \frac{K_\phi}{K_{\dot{\phi}}} p}{R\left[p^5 + \frac{1}{\tau_a} p^4 + \frac{1}{\tau_a} \frac{K_\phi}{K_{\dot{\phi}}} p^3 + \frac{1}{\tau_a} \frac{K_\sigma}{K_{\dot{\phi}}} \frac{Gg}{V} p^2 + \left(\frac{1}{\tau_a} \frac{K_I}{K_{\dot{\phi}}} \frac{Gg}{V} + \frac{1}{\tau_a} \frac{K_\sigma}{K_{\dot{\phi}}} \frac{Gg}{R}\right) p + \frac{1}{\tau_a} \frac{K_I}{K_{\dot{\phi}}} \frac{Gg}{R}\right]} \tag{A24}$$

The time variation of resultant target acceleration A_B in the horizontal plane required to produce a sinusoidally varying acceleration component in the plane of the wings of the interceptor may be expressed by the equation

$$A_B(t) = \frac{a_{B_m} \sin \omega t}{\cos \phi_F(t)} \tag{A25}$$

The amplitude and phase relationship of a_B and ϕ_F for particular values of frequency ω and amplitude a_{B_o} may be obtained by simultaneous solution of equations (A19) to (A23) for the transfer function $\frac{\phi_F}{a_B}$. The time variation of A_B was then obtained through use of equation (A25). This was done for several cases of frequency of target maneuver and magnitude of target acceleration and it was found that the resulting variation of A_B with time was only slightly distorted from a true sine wave for most combinations of frequency and amplitude. Within the range of the analysis the most distorted case was found at a frequency of 0.4 radian/sec and an amplitude of a_B of 0.75g and this case is presented in figure 18.

System with error differentiation.- The assumed system is shown in the block diagram presented as figure 17(b). Equations (A19), (A21), and (A23) also apply to this system, and in addition the following equation applies

$$\epsilon_2 = K_\sigma \sigma + K_D \frac{d\sigma}{dt} \tag{A26}$$

Transforming this equation gives

$$\epsilon_2(p) = K_\sigma \sigma(p) + K_D p \sigma(p)$$

Solving this equation and the transforms of equations (A19), (A21), and (A23) simultaneously for $\frac{\sigma(p)}{a_B(p)}$ gives

$$\frac{\sigma(p)}{a_B(p)} = \frac{p^2 + \frac{1}{\tau_a} p}{R\left[p^4 + \frac{1}{\tau_a} p^3 + \frac{1}{\tau_a} \frac{K_D}{K_{\ddot{\phi}}} \frac{Gg}{V} p^2 + \left(\frac{1}{\tau_a} \frac{K_D}{K_{\ddot{\phi}}} \frac{Gg}{R} + \frac{1}{\tau_a} \frac{K_\sigma}{K_{\ddot{\phi}}} \frac{Gg}{V}\right)p + \frac{1}{\tau_a} \frac{K_\sigma}{K_{\ddot{\phi}}} \frac{Gg}{R}\right]} \tag{A27}$$

System with filtered input differentiation.- The assumed system with filtered input differentiation is shown in figure 17(c). For this system equations (A19), (A21), and (A23) still apply, and in addition

$$\omega_{LS} = \frac{1}{R}\int_0^t (a_B - a_F)dt \tag{A28}$$

$$\epsilon_1 = K_\sigma \sigma + K_D \bar{\omega}_{LS} \tag{A29}$$

$$\bar{\omega}_{LS} + \tau_f \dot{\bar{\omega}}_{LS} = \omega_{LS} \tag{A30}$$

Transforming these equations into the Laplace domain gives

$$\omega_{LS}(p) = \frac{1}{R}\left(\frac{a_B(p)}{p} - \frac{a_F(p)}{p}\right)$$

$$\epsilon_1(p) = K_\sigma \sigma(p) + K_D \bar{\omega}_{LS}(p)$$

$$\bar{\omega}_{LS}(p) + \tau_f p \bar{\omega}_{LS}(p) = \omega_{LS}(p)$$

Solving these equations simultaneously with the transformed form of equations (A19), (A21), (A22), and (A23) gives

$$\frac{\sigma(p)}{a_B(p)} = \frac{p^3 + \left(\frac{1}{\tau_a} + \frac{1}{\tau_f}\right)p^2 + \left(\frac{1}{\tau_a \tau_f} + \frac{1}{\tau_a} \frac{K_\phi}{K_{\ddot{\phi}}}\right)p}{R\left[p^5 + \left(\frac{1}{\tau_a} + \frac{1}{\tau_f}\right)p^4 + \left(\frac{1}{\tau_a \tau_f} + \frac{1}{\tau_a} \frac{K_\phi}{K_{\ddot{\phi}}}\right)p^3 + \left(\frac{1}{\tau_a} \frac{K_\sigma}{K_{\ddot{\phi}}} \frac{Gg}{V} + \frac{1}{\tau_a \tau_f} \frac{K_\phi}{K_{\ddot{\phi}}}\right)p^2 + \frac{Gg}{\tau_a \tau_f}\left(\frac{K_\sigma}{K_{\ddot{\phi}}} \frac{1}{V} + \frac{K_\sigma}{K_{\ddot{\phi}}} \frac{\tau_f}{R} + \frac{K_D}{K_{\ddot{\phi}}} \frac{1}{R}\right)p + \frac{1}{\tau_a \tau_f} \frac{K_\sigma}{K_{\ddot{\phi}}} \frac{Gg}{R}\right]} \tag{A31}$$

APPENDIX B

EFFECT OF USE OF FILTERED INPUT DIFFERENTIATION ON LEVEL OF NOISE INPUT TO TIE-IN SYSTEM

The results of ground-to-air tracking tests of the radar used in the subject interceptor are presented in reference 4. These results show that the power spectral density (PSD) of the radar tracking error (noise) for a head-on aspect of the target can be well approximated by the expression

$$(\mathrm{PSD})_{n_\sigma} = \frac{K_{n_\sigma}}{1 + \beta\omega^2} \tag{B1}$$

Although data for a tail aspect were not obtained, it is believed that the foregoing expression would represent adequately the frequency variation of the noise for the tail aspect.

The antenna position signal goes to the tie-in in practically unfiltered form so that the noise input to the tie-in from this source is given by the following expression:

$$K_\sigma(\mathrm{PSD})_{n_\sigma} = \frac{K_\sigma K_{n_\sigma}}{1 + \beta\omega^2} \tag{B2}$$

The amplitude of the transfer function relating antenna rate to antenna position is simply ω and so the power spectral density (PSD) of the noise on the antenna rate signal is

$$(\mathrm{PSD})_{n_{\dot\sigma}} = K_{n_\sigma} \frac{\omega^2}{1 + \beta\omega^2} \tag{B3}$$

In the present application this signal is filtered before being applied as an input to the tie-in, and the power spectrum of this noise signal is given by

$$K_D(\mathrm{PSD})_{n_{\dot\sigma}} = K_D K_{n_\sigma} \frac{\omega^2}{\left(1 + \beta\omega^2\right)\left[\left(1 + (\tau_f\omega)^2\right)\right]} \tag{B4}$$

The root-mean-square (rms) values of the noise signal to the tie-in may be determined by integrating the area under the power-spectral-density

curve and taking the square root of the result. This operation may be expressed analytically as follows:

$$\text{rms} = \sqrt{\int_0^\infty \text{PSD}\, d\omega} \tag{B5}$$

For the noise at the tie-in associated with radar antenna-position errors this becomes

$$\text{rms} = \sqrt{\int_0^\infty \frac{K_\sigma K_{n_\sigma}}{1 + \beta\omega^2}\, d\omega}$$

$$= \sqrt{\frac{\pi}{2} \frac{K_\sigma K_{n_\sigma}}{\sqrt{\beta}}} \tag{B6}$$

For the noise at the tie-in associated with radar antenna-rate errors

$$\text{rms} = \sqrt{\frac{\pi}{2} \frac{K_D K_{n_\sigma}}{\beta - \tau_f^2}\left(\frac{1}{\tau_f} - \frac{1}{\sqrt{\beta}}\right)} \tag{B7}$$

The ratio of the noise produced by the filtered rate signal to the noise produced by the position signal therefore is

$$\frac{\text{rms}_{n_{\dot\sigma}}}{\text{rms}_{n_\sigma}} = \sqrt{\frac{K_D}{K_\sigma} \frac{1}{\left(\beta - \tau_f^2\right)}\left(\frac{\sqrt{\beta}}{\tau_f} - 1\right)} \tag{B8}$$

The value of β for the test radar as obtained from the results of reference 4 is 0.18. By use of this value the noise parameter

$$\frac{\text{rms}_{n_{\dot\sigma}}}{\text{rms}_{n_\sigma}} \sqrt{\frac{K_\sigma}{K_D}}$$

is plotted against the filter time constant in figure 19. For the flight tests of the system with filtered input differentiation the value of $\sqrt{\frac{K_\sigma}{K_D}}$ was about 0.4, and with the filter time constant of 1.4 seconds used in the flight tests the ratio of the noise associated with the input rate

signal to that associated with the antenna position signal is slightly over 1.5. For a filter time constant of 1 second (used in the analytical study) this ratio would be slightly over 2.

This analysis can also be applied to the system with error differentiation. In this case the ratio of the root-mean-square noise associated with the differentiated error signal to the root-mean-square noise associated with the antenna position signal would be the same relationship presented in equation (B8). Since there is no filtering of the differentiated error signal, this ratio would be infinite. It is probable that some filtering could be applied; however, filter time constants of the magnitude required to reduce the ratio to moderate values (for example, 4) would introduce lags which would detrimentally affect the stability of the tracking loop.

REFERENCES

1. Brown, Gordon S., and Campbell, Donald P.: Principles of Servomechanisms. John Wiley & Sons, Inc., 1948.

2. Woodling, C. H., and Gates, Ordway B., Jr.: Theoretical Analysis of the Longitudinal Behavior of an Automatically Controlled Supersonic Interceptor During the Attack Phase Against Maneuvering and Nonmaneuvering Targets. NACA RM L55G18, 1955.

3. Lusian, R. G., and Blattner, C. J.: F2H-3 Airframe Dynamic Lateral and Longitudinal Stability Characteristics Determined From Flight Test - Automatic Fire Control Program. Rep. No. 3091 (Contract No. NOa(s)-51-023), McDonnell Aircraft Corp., Oct. 22, 1953.

4. Schillinger, E. J.: Ground-to-Air Tracking Tests of the Westinghouse AN/APQ-41 Radar. Rep. No. 3183 (Contract No. NOa(s)-51-023), McDonnell Aircraft Corp., July 9, 1953.

5. Blattner, C. J., and Golding, N. J., Jr.: Automatic Fire Control System - F2H-3 Banshee. Final Report. Rep. No. 3440 (Contract No. NOa(s)51-023), McDonnell Aircraft Corp., Oct. 15, 1954.

6. Anon.: Handbook Maintenance Instructions - Navy Model F2H-3, -4 Airplanes. AN 01-245FBC-2, U. S. Air Force and Bur. Aero., Aug. 1, 1953 (Revised Apr. 1, 1954).

7. Rathert, George A., Jr., Gadeberg, Burnett L., and Ziff, Howard L.: An Analysis of the Tracking Performance of Two Straight-Wing and Two Swept-Wing Fighter Airplanes With Fixed Sights in a Standardized Test Maneuver. NACA RM A53H12, 1953.

8. Gardner, Murray F., and Barnes, John L.: Transients in Linear Systems Studied by the Laplace Transformation. Lumped-Constant Systems. Vol. I, John Wiley & Sons, Inc., 1942.

9. Anon.: Flyability of the Aero 13 Armament Control System. Contract No. NOa(s) 52-1101, Westinghouse Elec. Corp., Air Arm Div. (Baltimore, Md.), June 28, 1954.

10. Mathews, Charles W.: Study of the Attack of an Automatically Controlled Interceptor on a Maneuvering Bomber With Emphasis on Proper Coordination of Lift-Acceleration and Roll-Angle Commands During Rolling Maneuvers. NACA RM L54E27, 1954.

TABLE I

DIMENSIONAL AND MASS CHARACTERISTICS OF FLIGHT-TEST VEHICLE

Overall length, ft	48.04
Wing:	
Span, ft	41.70
Area, sq ft	294.0
Section, wing-fold	NACA 65_1-212
Incidence, deg	-0.5
Aspect ratio	5.9
Dihedral, deg	3.0
Mean aerodynamic chord, in.	88.4
Leading-edge sweepback, in.	0
Ailerons:	
Mean chord rearward of hinge line, ft	1.24
Span, percent b/2	32.8
Horizontal-tail surfaces:	
Total area, sq ft	70.1
Span, ft	17.8
Elevator area rearward of hinge line, sq ft	18.7
Distance from $0.256\bar{c}$ to elevator hinge line, ft	24.0
Dihedral, deg	10.0
Vertical-tail surfaces:	
Total area, sq ft	39.9
Rudder area rearward of hinge line, sq ft	9.6
Distance from $0.256\bar{c}$ to rudder hinge line, ft	22.2
Approximate weight at flight-test conditions, lb	20,700
Relative density, (20,000 ft)	41.6
Center-of-gravity station, percent mean aerodynamic chord	25.7
Moment of inertia about X-axis, I_X, slug-ft^2	15,145
Moment of inertia about Y-axis, I_Y, slug-ft^2	41,677
Moment of inertia about Z-axis, I_Z, slug-ft^2	54,616

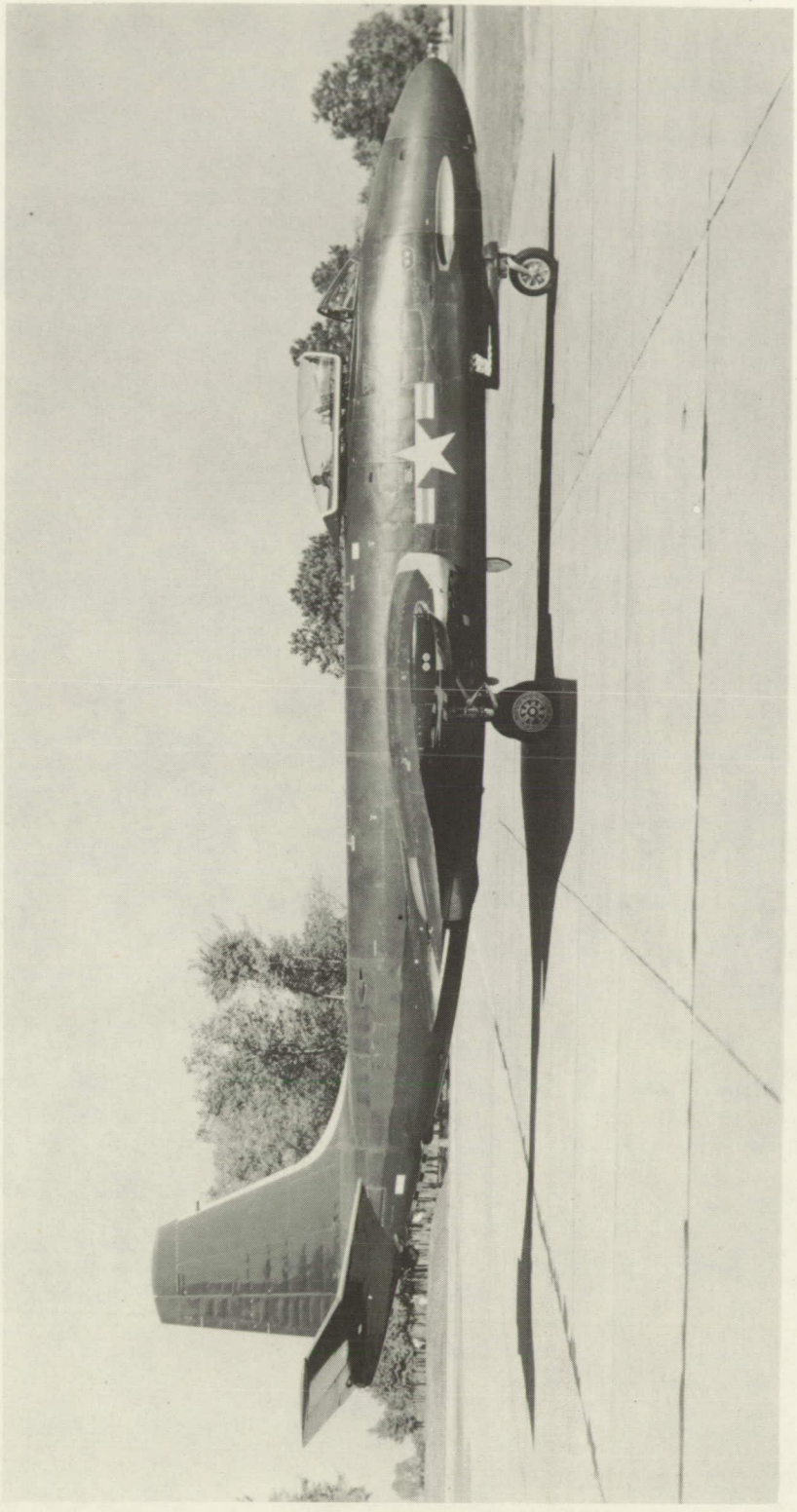

L-91217.1

Figure 1.- Side view of flight-test airplane.

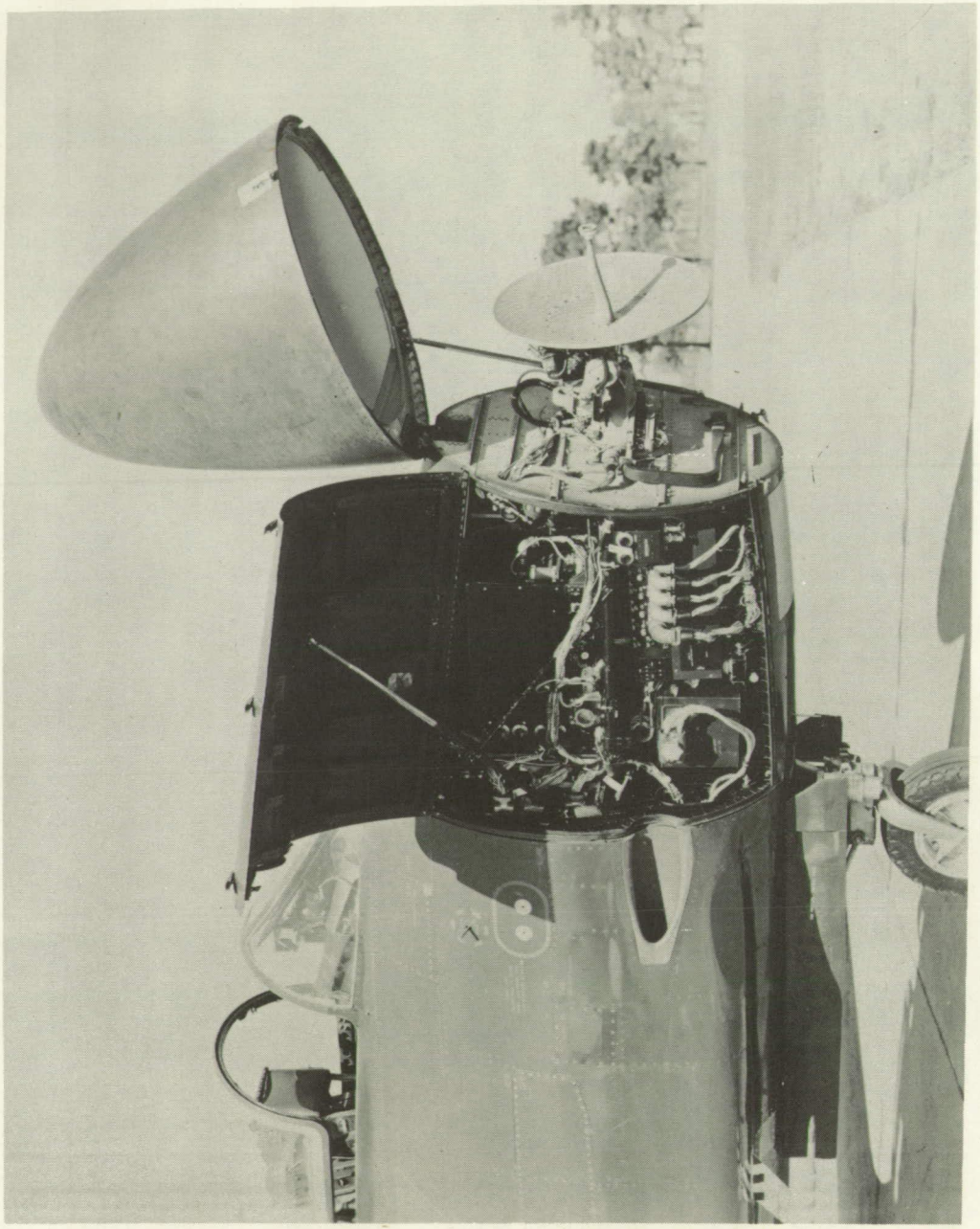

L-91233.1

Figure 2.- Radar and computer components of fire-control system.

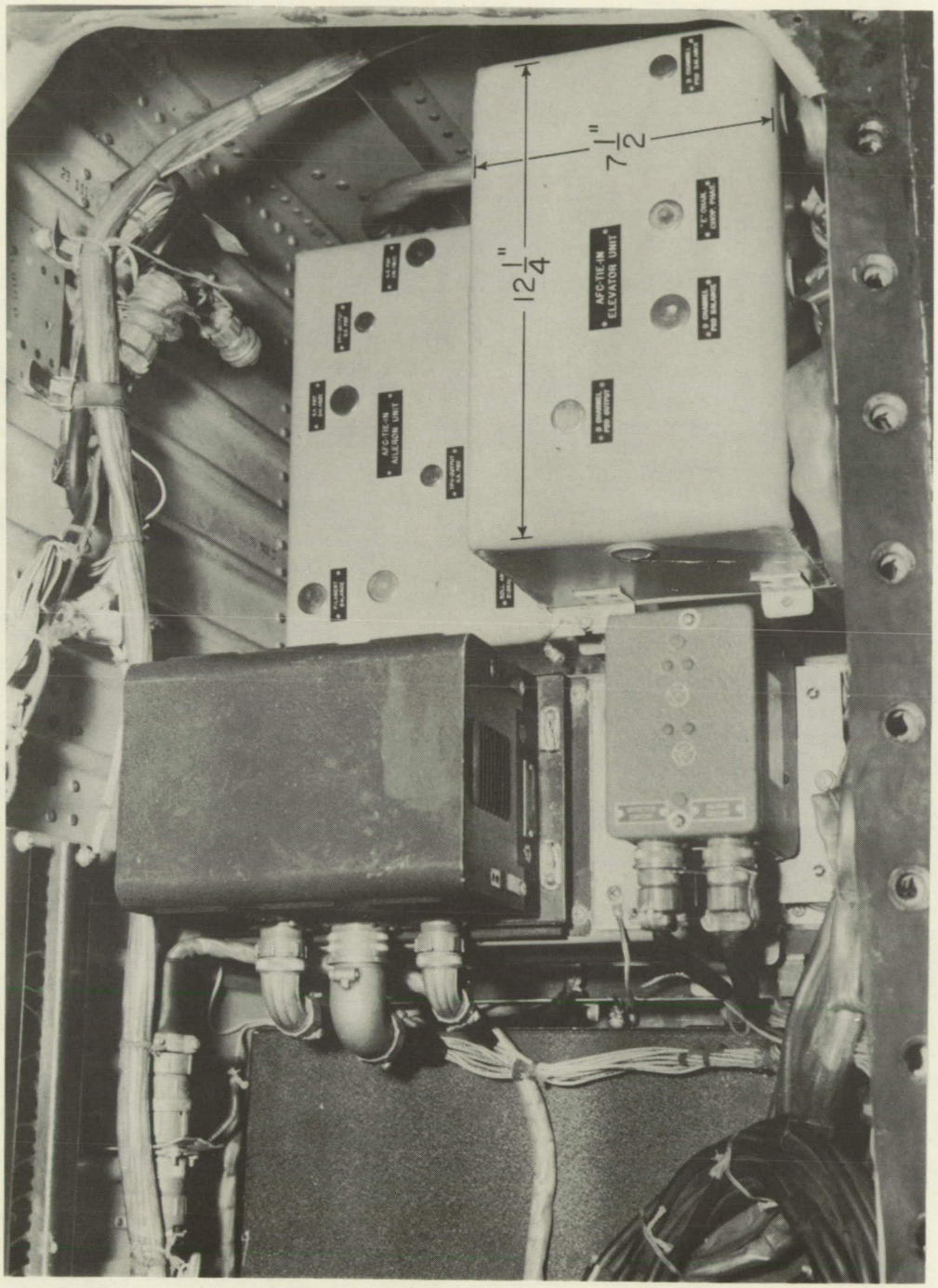

L-86788.1

Figure 3.- Tie-in components located in well in left wing of flight-test airplane.

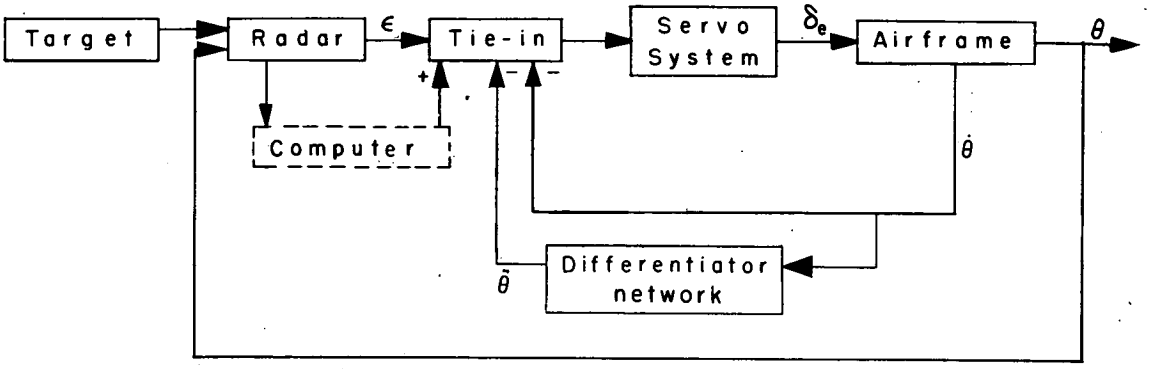

(a) Elevation channel.

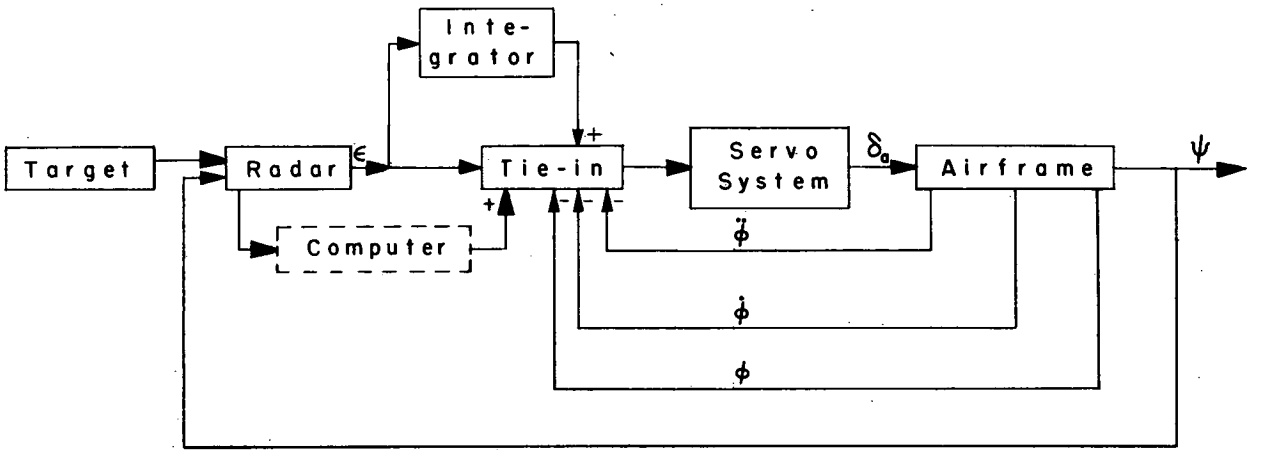

(b) Deflection channel.

Figure 4.- Block diagram of elevation channel and deflection channel of automatic interceptor system.

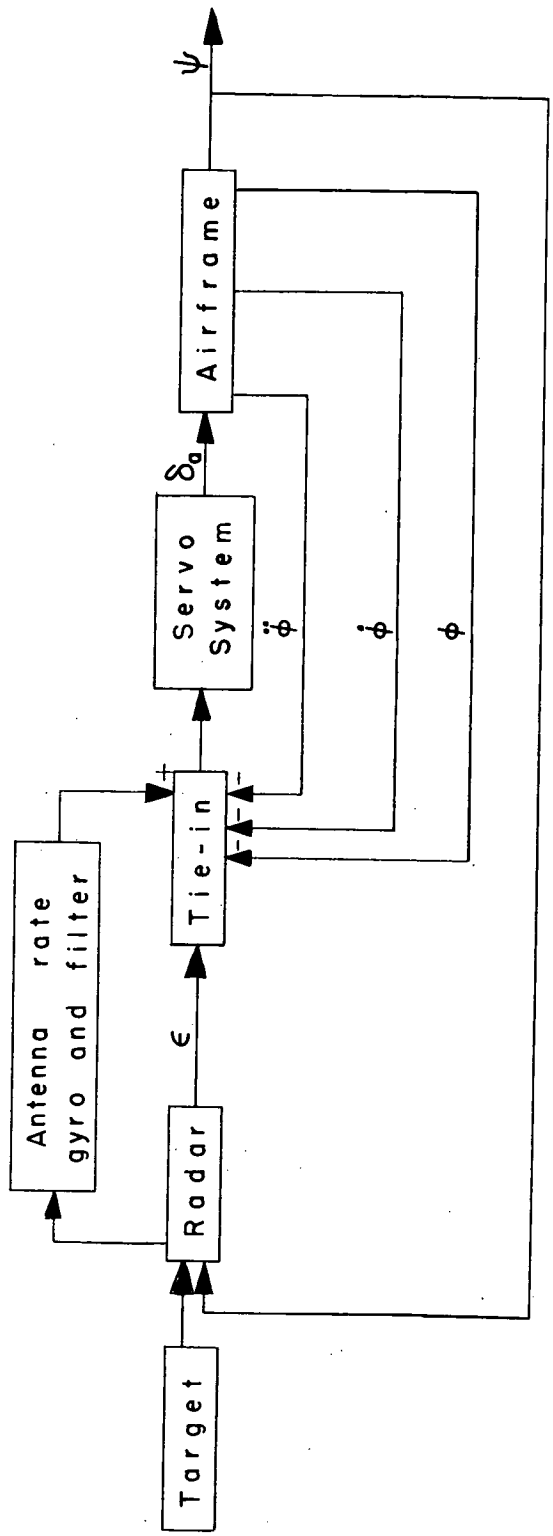

Figure 5.- Block diagram of modified deflection channel of the interceptor system.

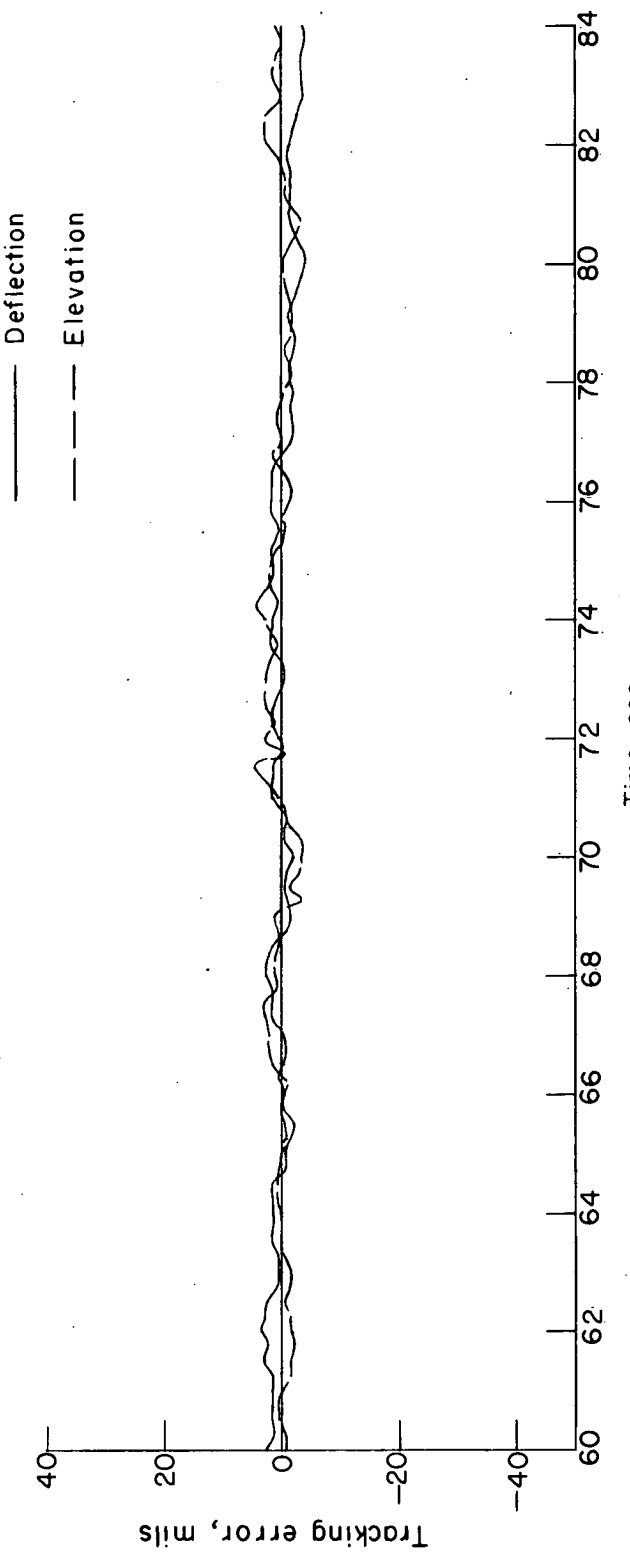

Figure 6.- Time history of tracking errors during tail-chase tracking of nonmaneuvering target.

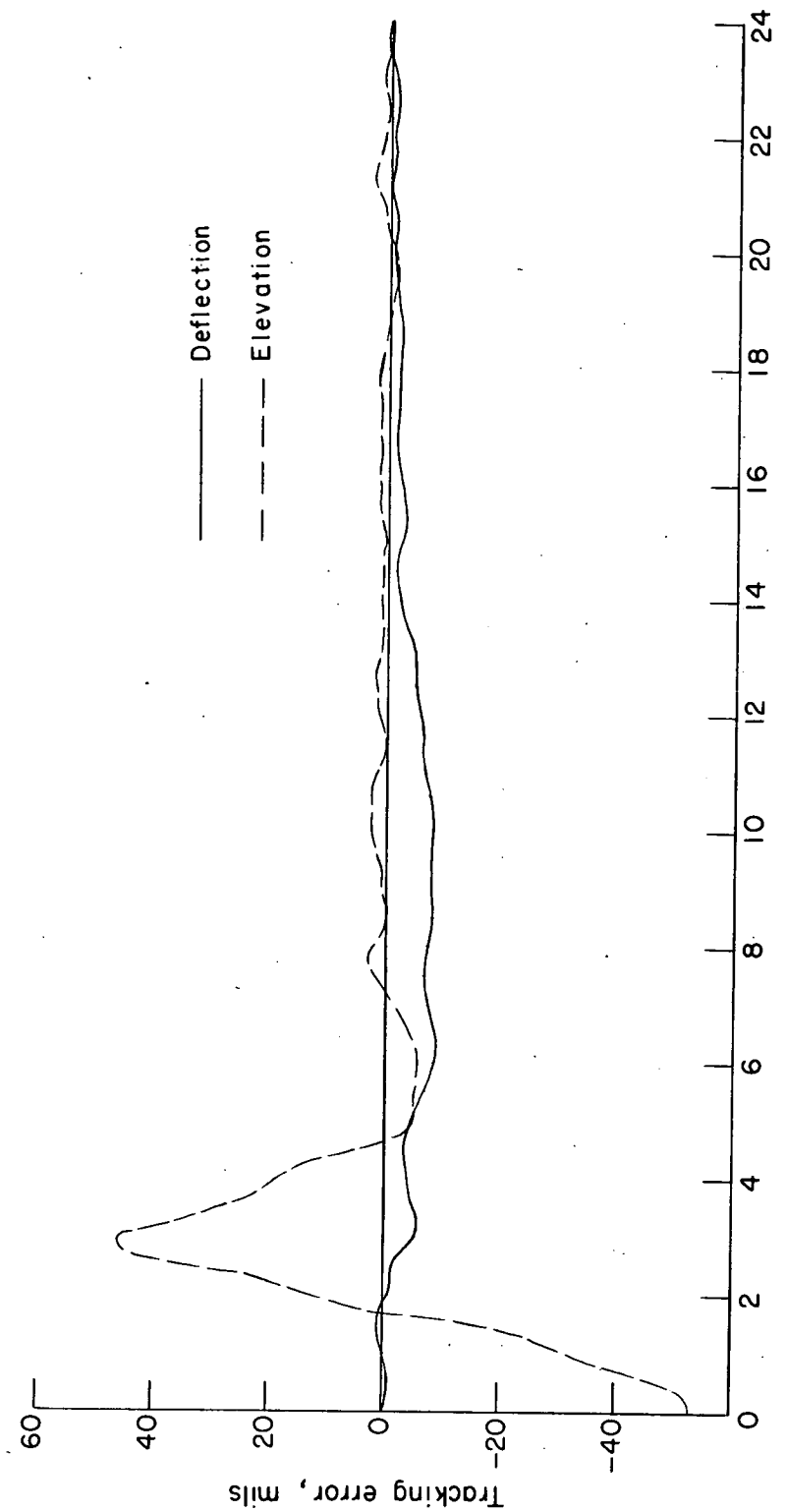

Figure 7.- Time history of tracking errors following an engagement of automatic interceptor system with initial elevation error. Nonmaneuvering target.

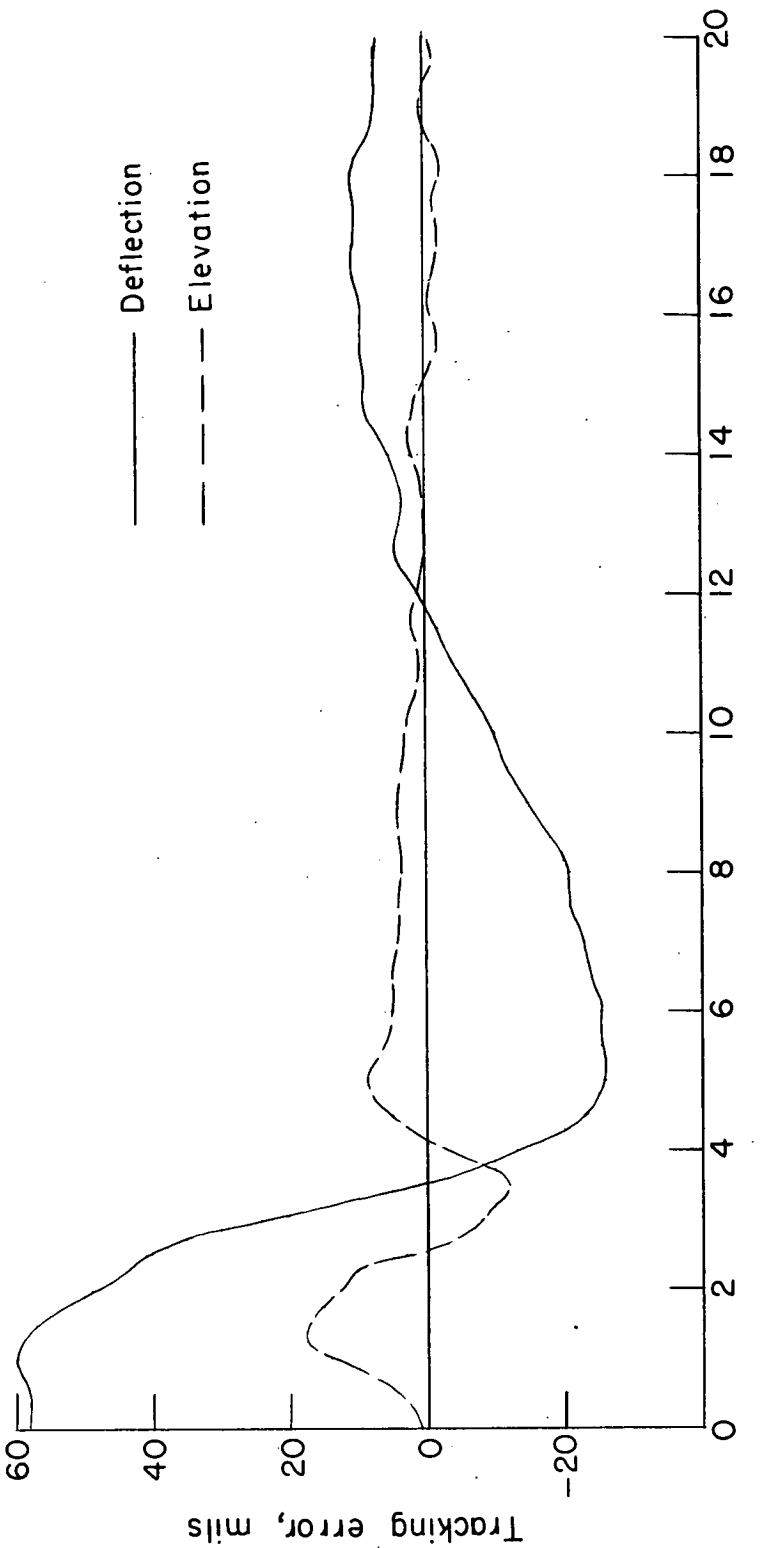

Figure 8.- Time history of tracking errors following an engagement of automatic interceptor system with an initial deflection error. Nonmaneuvering target.

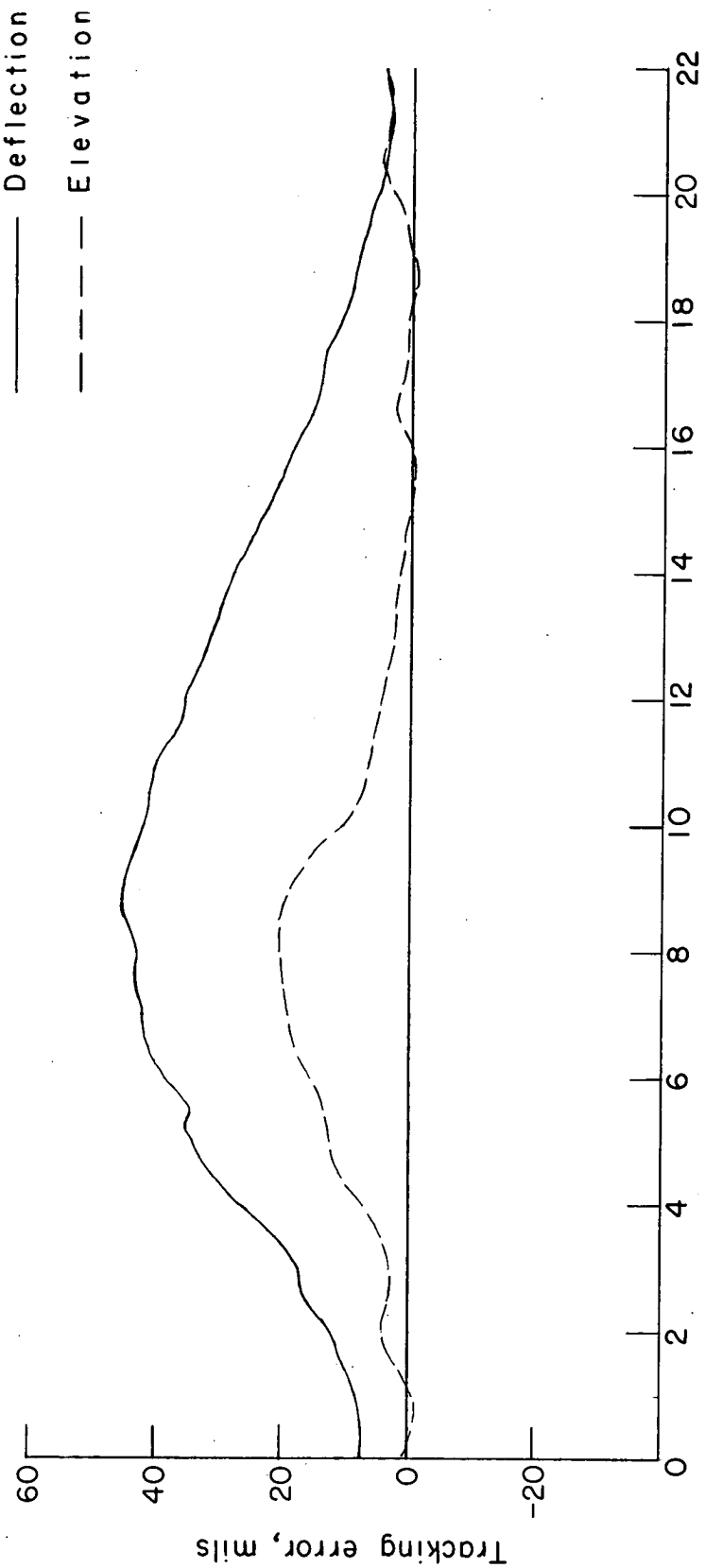

Figure 9.- Time history of tracking errors following target entry into steady turn.

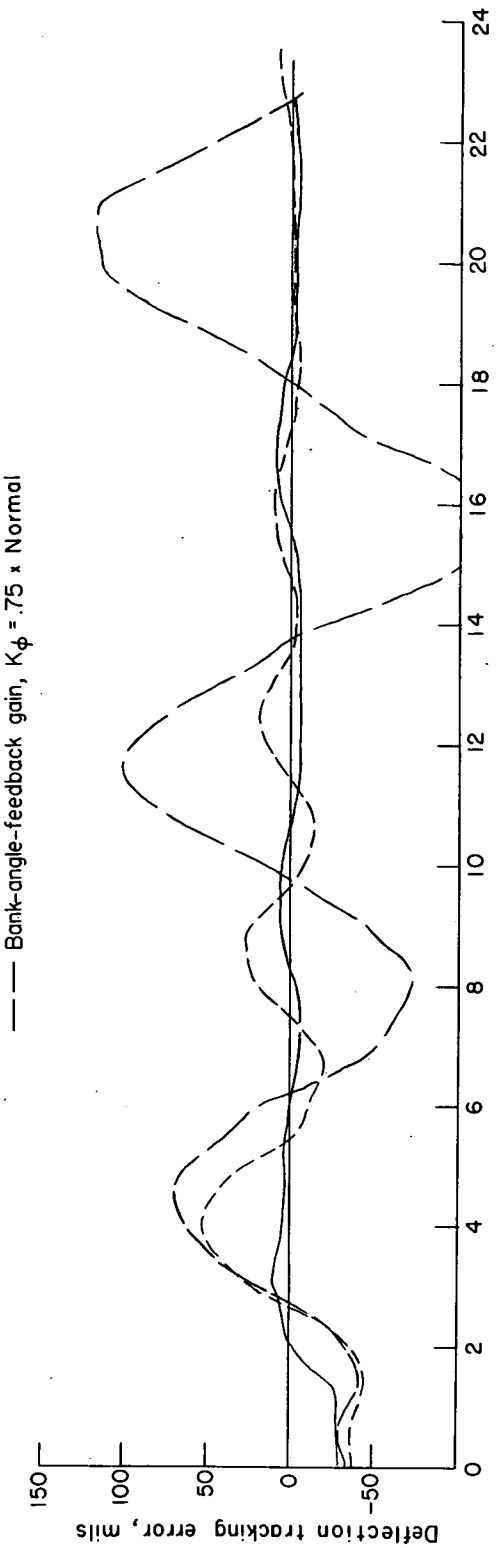

Figure 10.- Time histories of deflection tracking errors following engagements of interceptor system with initial deflection error where different forward loop gains were used.

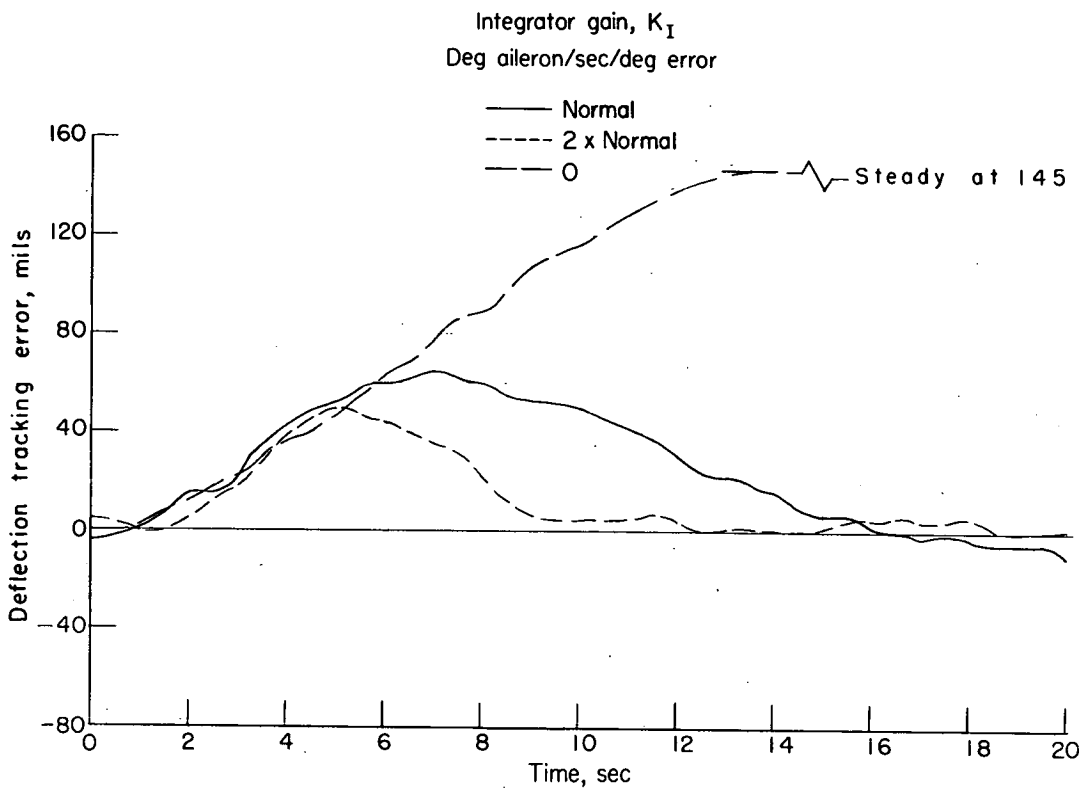

(a) Response to target turn.

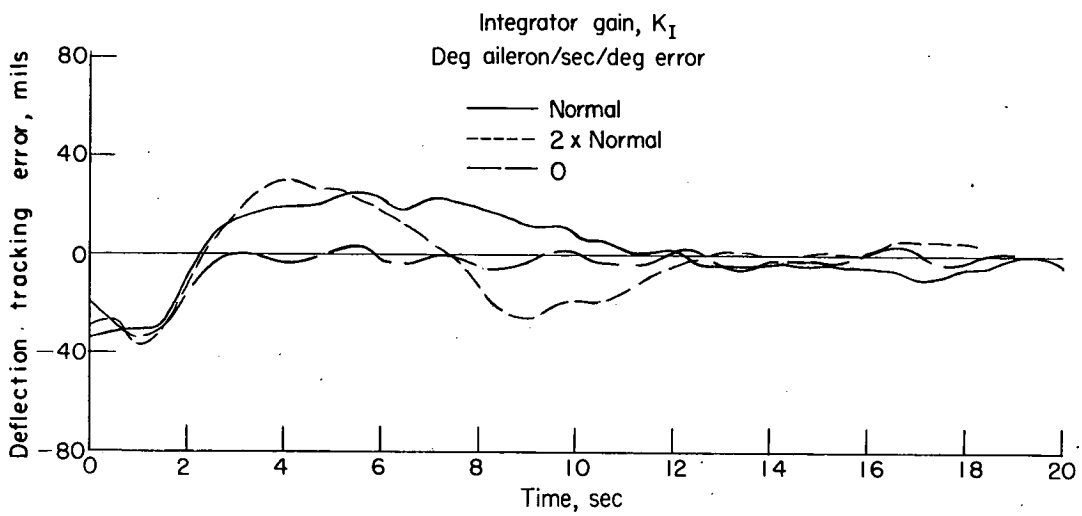

(b) Response following an engagement with an initial deflection error.

Figure 11.- Effect of integrator gain upon deflection tracking error.

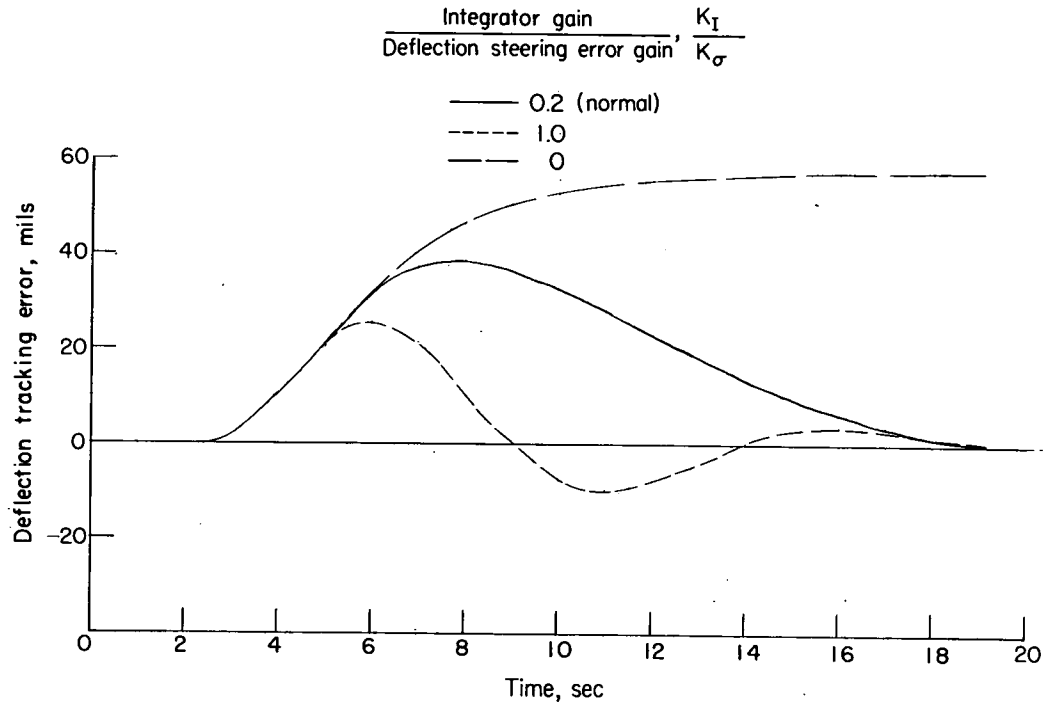

(a) Response to input approximating a target turn.

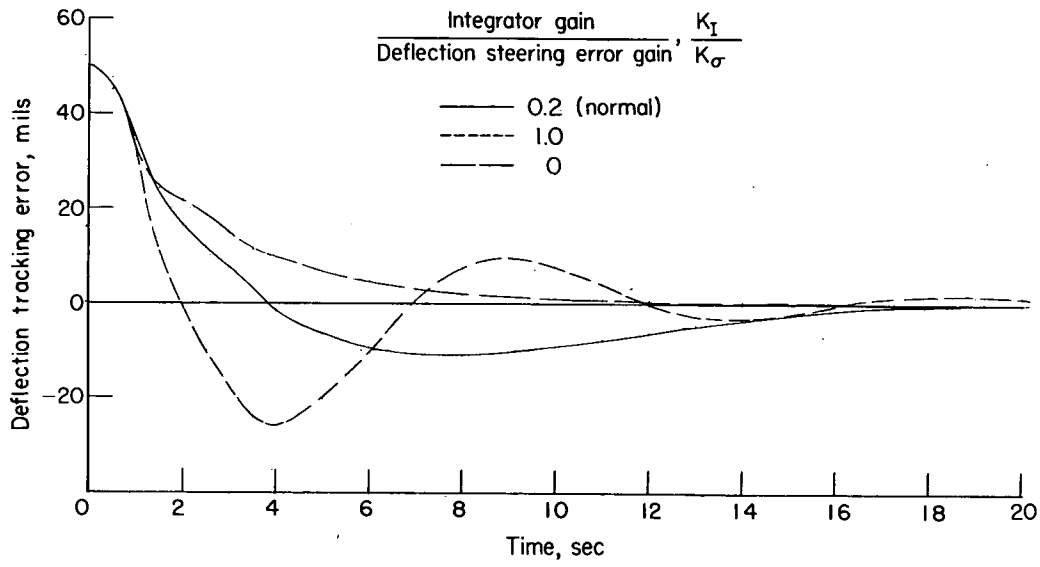

(b) Response to engagement with initial deflection error.

Figure 12.- Effects of integrator gain upon computed deflection tracking of simplified deflection channel.

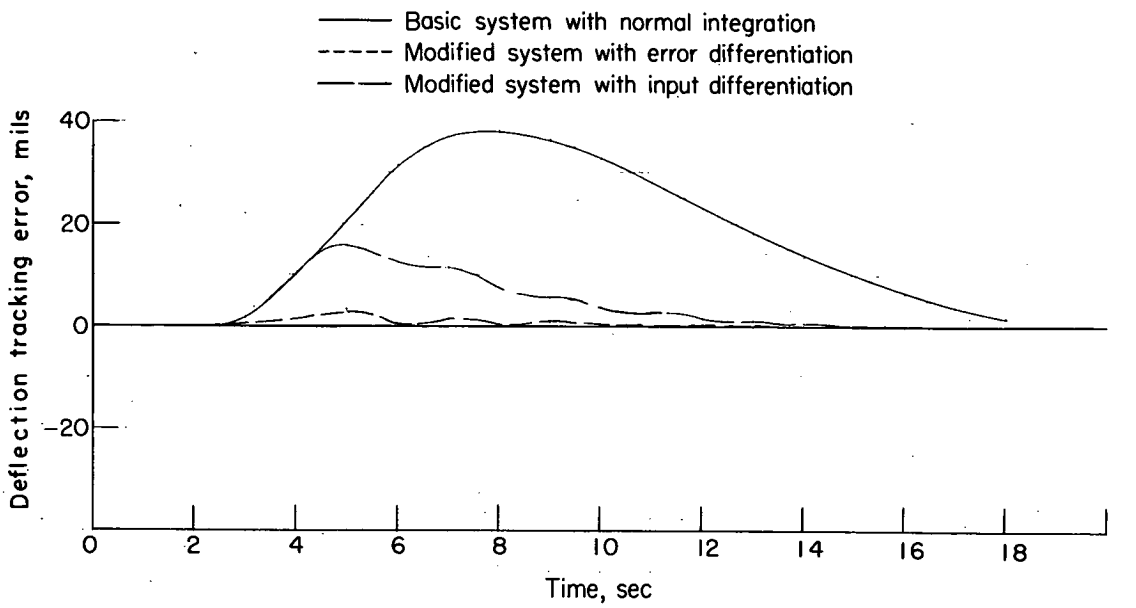

(a) Response to input approximating a target turn.

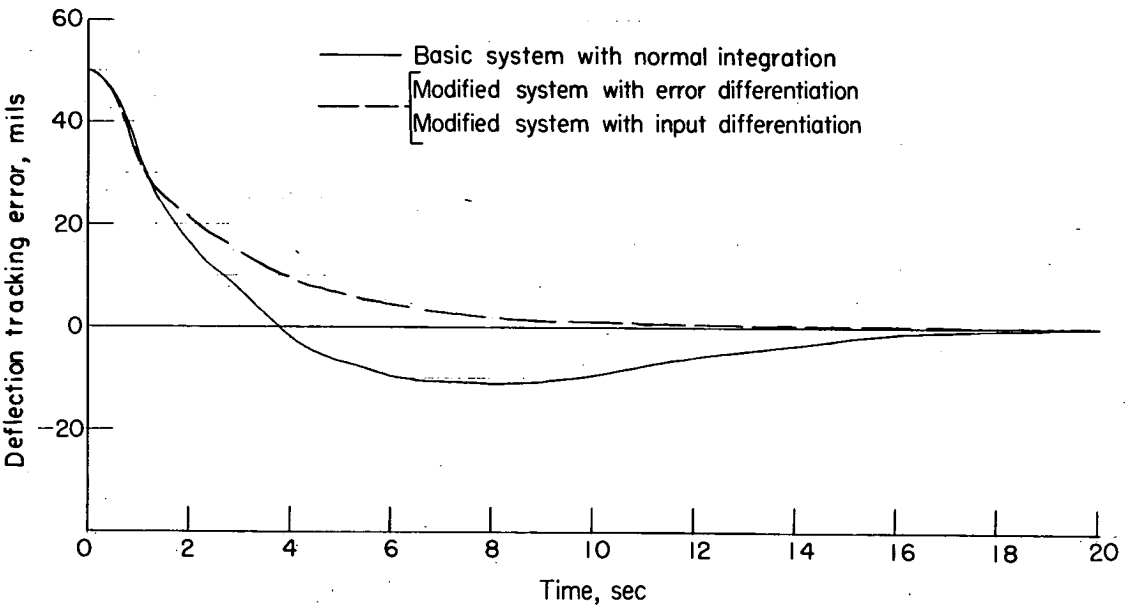

(b) Response to engagement with intial deflection error.

Figure 13.- Computed deflection tracking of modified deflection channel with error differentiation.

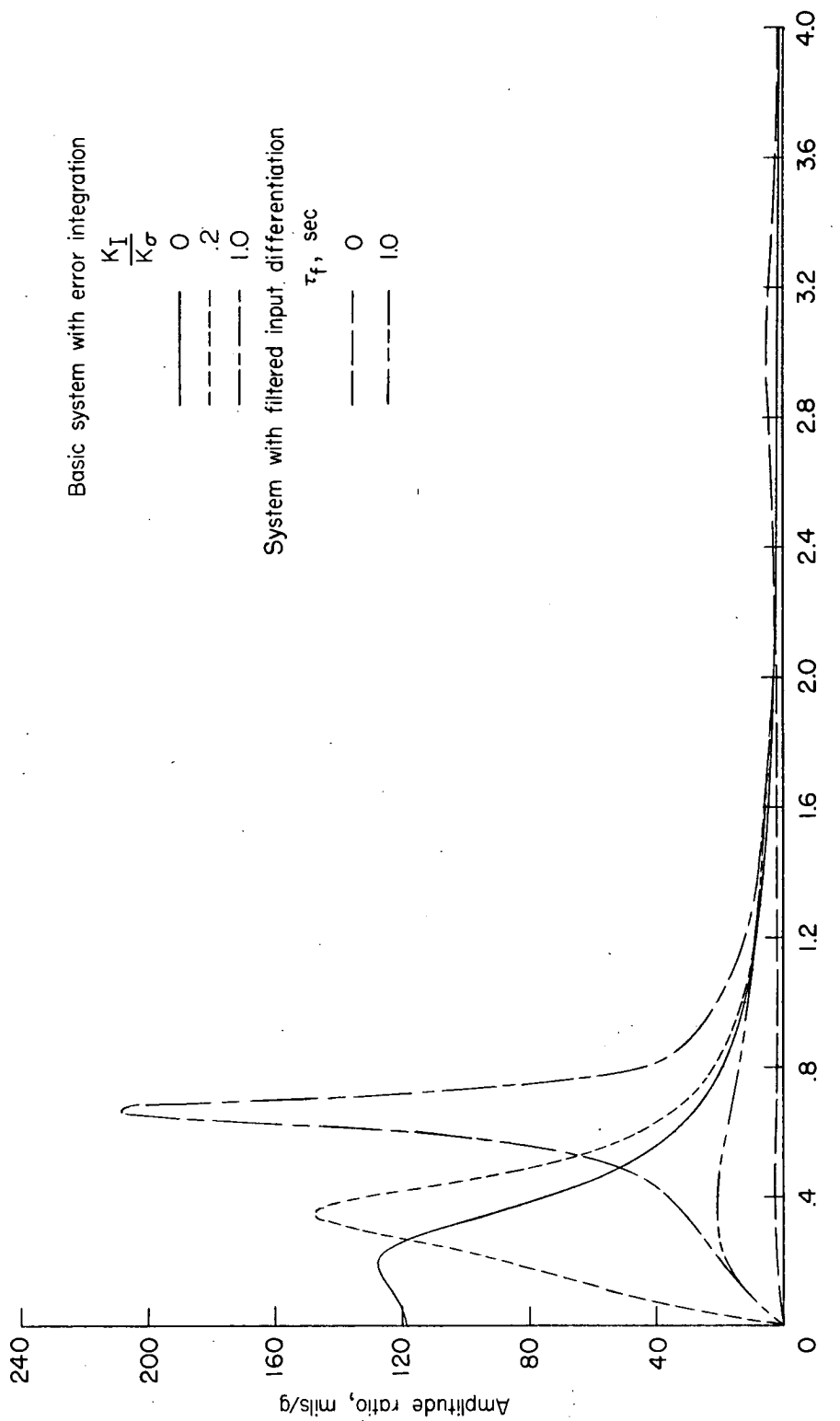

Figure 14.- Calculated ratio of amplitude of deflection tracking error to target acceleration as a function of frequency of target oscillation.

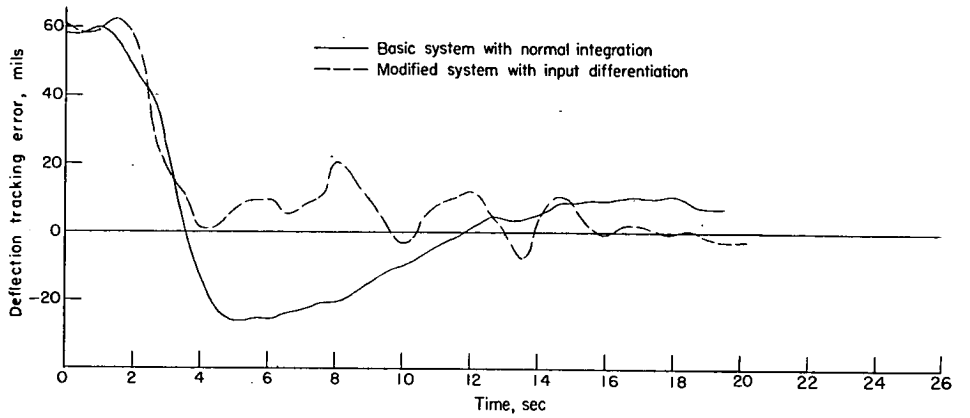

(a) Response following an engagement with an initial deflection error.

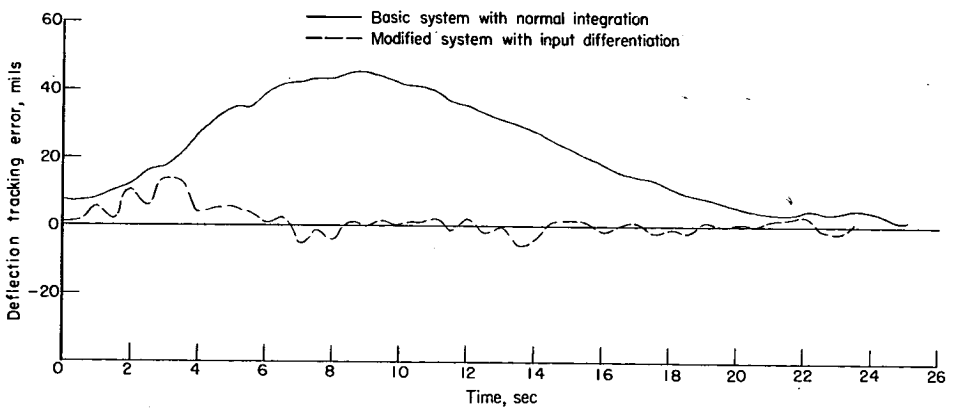

(b) Response to target turn.

Figure 15.- Comparison of flight time histories of deflection tracking error of modified interceptor system with filtered input differentiation and basic system.

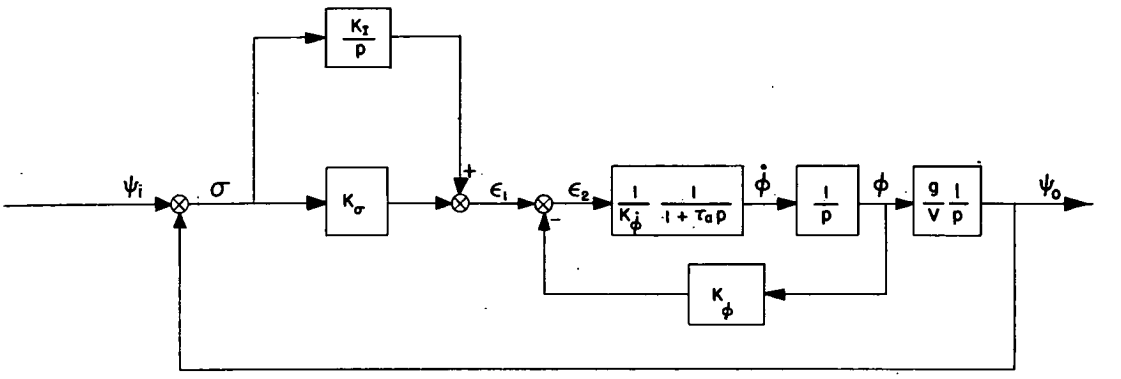

(a) Deflection channel.

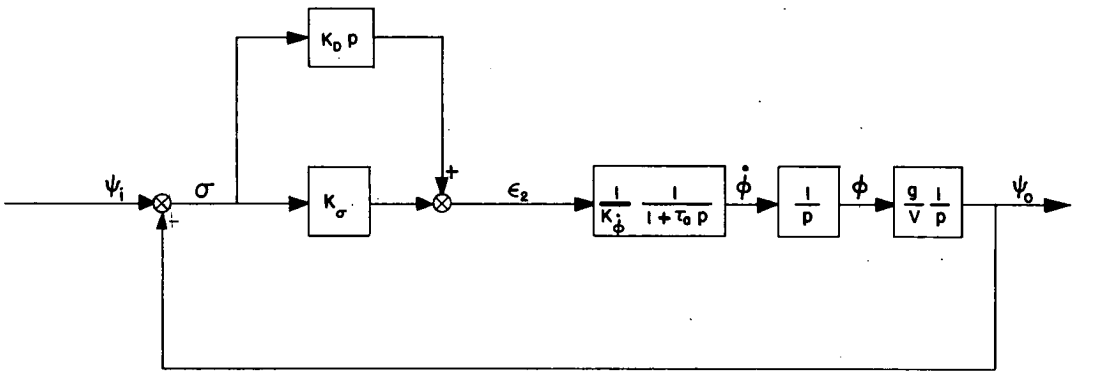

(b) Error differentiation deflection channel.

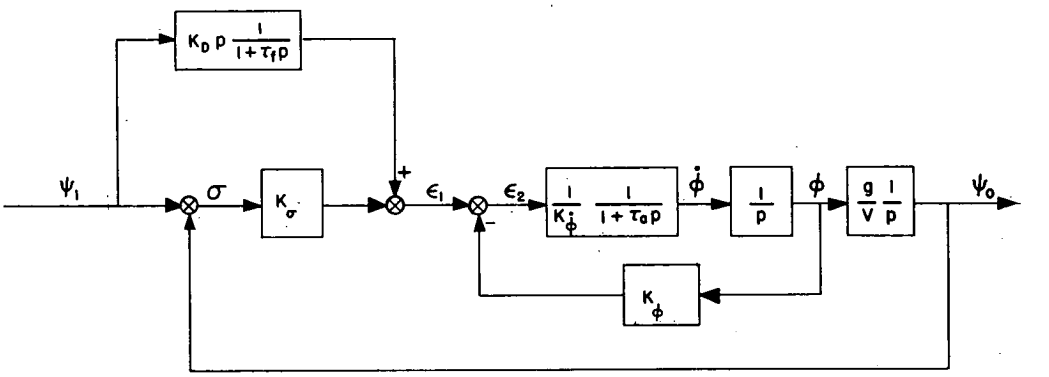

(c) Filtered-input differentiation system.

Figure 16.- Block diagram of simplified version of deflection channel, error differentiation deflection channel, and simplified version of filtered input differentiation system of interceptor system.

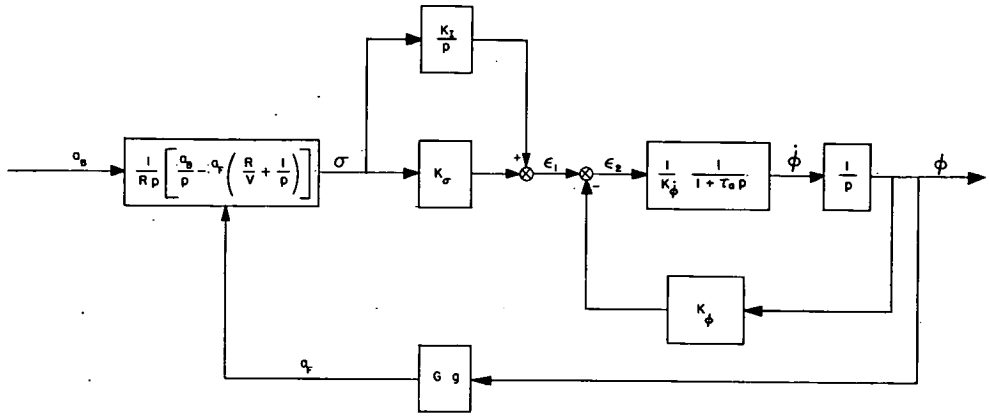

(a) Deflection channel.

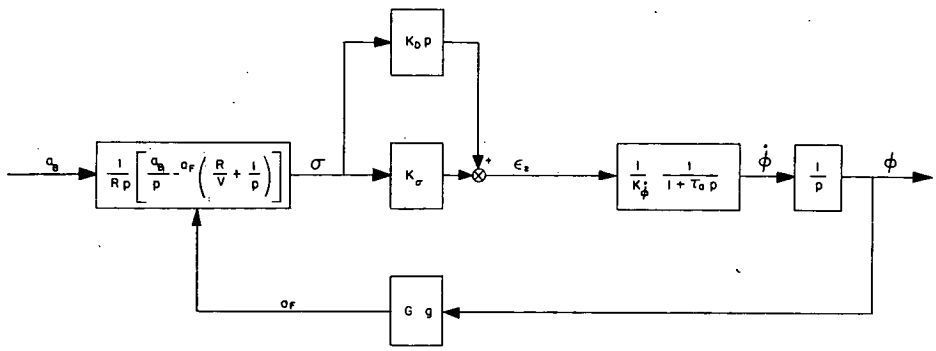

(b) Error differentiation system.

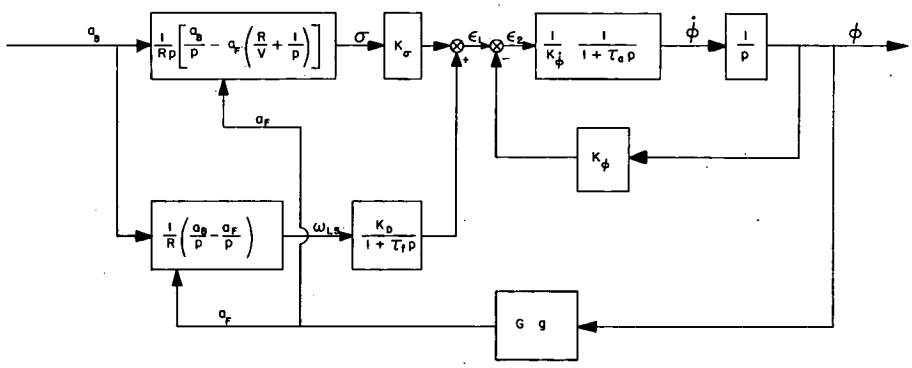

(c) Filtered input differentiation system.

Figure 17.- Block diagram of simplified deflection channel error differentiation system and filtered input differentiation system assumed for frequency-response analysis.

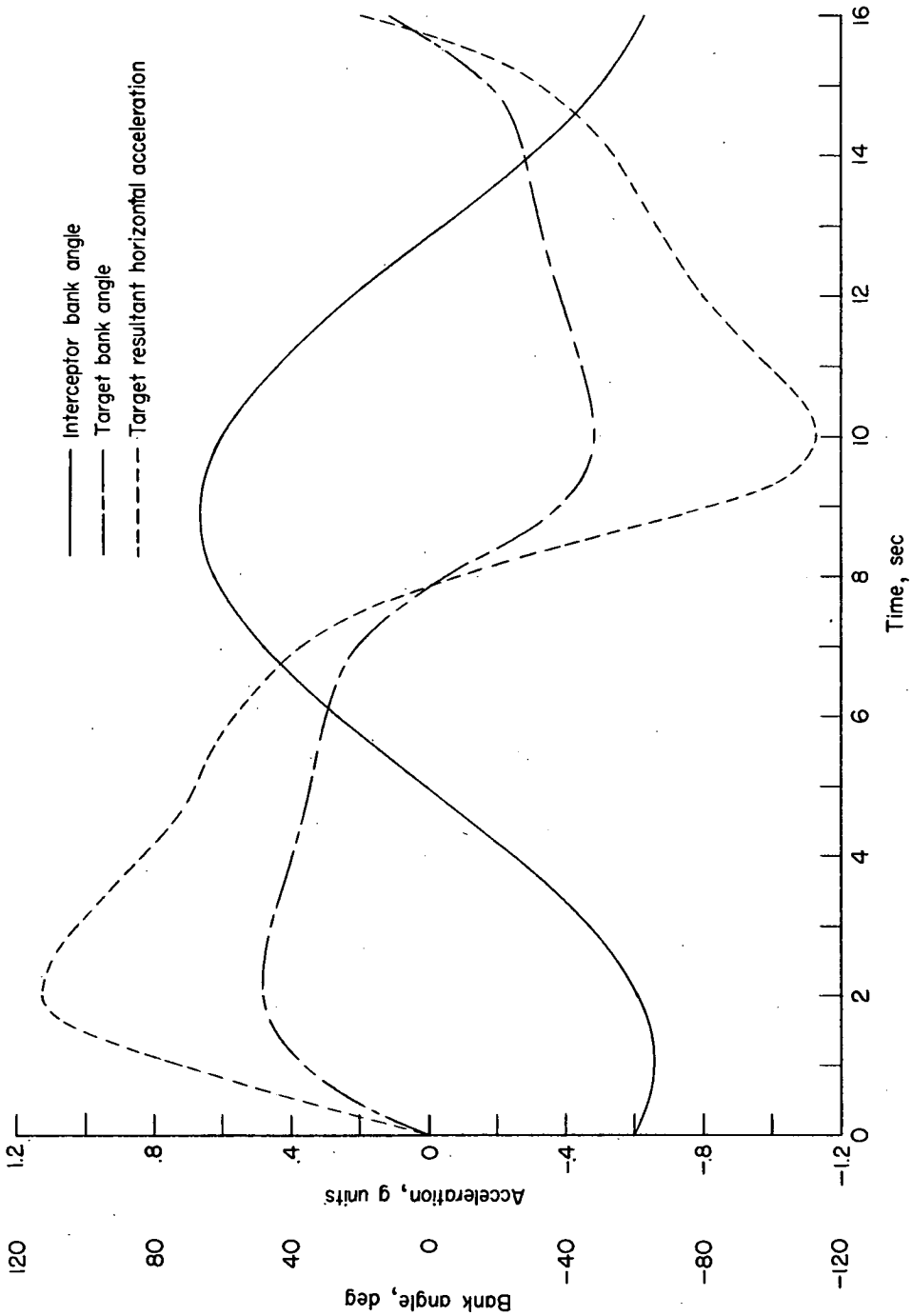

Figure 18.- Calculated time histories of target bank angle and normal acceleration required to produce a sinusoidally varying component of acceleration of 0.75g in the plane of the interceptors wings. Frequency, 0.4 radian/sec. Interceptor deflection channel is basic system with a normal integrator gain.

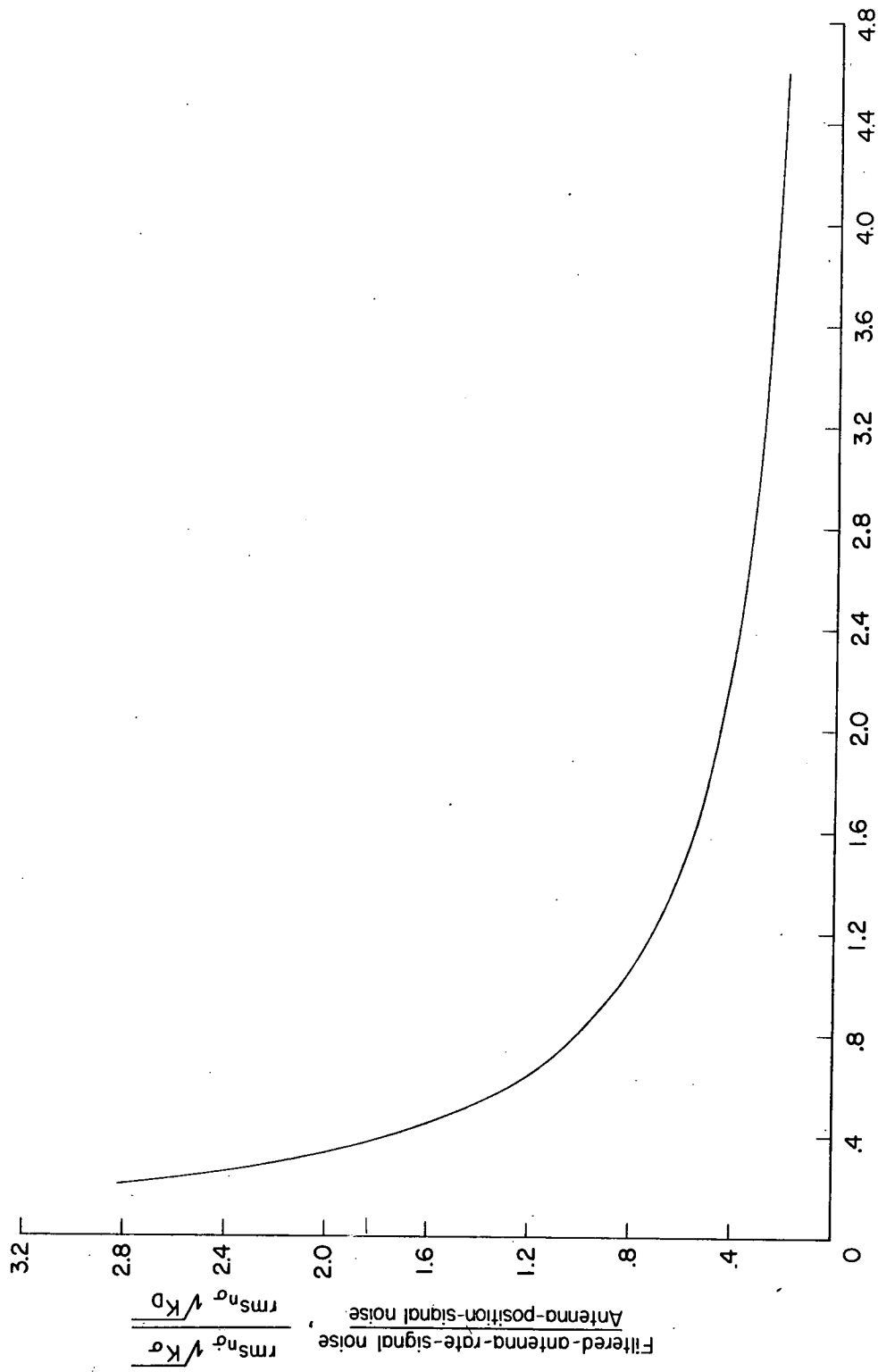

Figure 19.- Effect of filter time constant on ratio of filtered antenna-rate-signal noise and antenna-position-signal noise.

NACA - Langley Field, Va.